

**SYNCHRONOUS MACHINE MODELS FOR
SIMULATION OF INDUCTION MOTOR TRANSIENTS**

by

RICKY P. K. HUNG

B.A.Sc. (EE), The University of British Columbia, 1993

A THESIS SUBMITTED IN PARTIAL FULFILLMENT OF

THE REQUIREMENTS FOR THE DEGREE OF

MASTER OF APPLIED SCIENCE

in

THE FACULTY OF GRADUATE STUDIES

Department of Electrical Engineering

**We accept this thesis as conforming
to the required standard**

THE UNIVERSITY OF BRITISH COLUMBIA

April 1995

© Ricky P. K. Hung, 1995

In presenting this thesis in partial fulfilment of the requirements for an advanced degree at the University of British Columbia, I agree that the Library shall make it freely available for reference and study. I further agree that permission for extensive copying of this thesis for scholarly purposes may be granted by the head of my department or by his or her representatives. It is understood that copying or publication of this thesis for financial gain shall not be allowed without my written permission.

Department of ELECTRICAL ENGINEERING

The University of British Columbia
Vancouver, Canada

Date APRIL 26, 1995

ABSTRACT

The induction motor is the most common motor type used in industry. Analyzing its performance is either concerned with steady-state behavior, or the transient behavior during start-up and during system disturbances. Due to the advancement in power electronics, induction motors are now commonly used in adjustable-speed drives. The harmonic currents generated from these drives may result in voltage distortions and potential resonance problems. Computer simulations of induction motor performance are therefore more important than ever before. Although many simulation programs are available for induction motor studies, the Electromagnetic Transients Program (EMTP) is probably better than other simulation packages, because it contains detailed models of many other power system components, such as transformers, transmission lines and thyristors, which must be considered in certain types of motor simulations. This thesis presents a method of using the existing EMTP synchronous machine model to simulate induction motor transients. This approach allows simulations for both machine types using essentially the same program code. The data conversion algorithm, which converts standard motor specifications into equivalent circuit parameters, is explained. The steady-state initialization of an induction motor is discussed as well. The start-up of an induction motor is simulated using the proposed model. These simulation results are then compared with an independent program which uses a 4th-order Runge-Kutta solution method. It is observed that the results from the proposed model agree very well with the ones from the Runge-Kutta solution method.

TABLE OF CONTENTS

| | |
|---|------------|
| Abstract | ii |
| Table of Contents | iii |
| List of Tables | v |
| List of Figures | vi |
| Acknowledgment | vii |
| | |
| 1. INTRODUCTION | 1 |
| | |
| 2. SIMILARITY BETWEEN THE SYNCHRONOUS MACHINE AND INDUCTION MACHINE MODELS | 4 |
| | |
| 3. DATA CONVERSION | 7 |
| 3.1 Introduction | 7 |
| 3.2 Conversion Algorithm | 9 |
| | |
| 4. STEADY-STATE REPRESENTATION AND INITIALIZATION | 19 |
| 4.1 Introduction | 19 |
| 4.2 The Thevenin Equivalent Based Method | 20 |
| 4.3 The Compensation Based Method | 25 |
| 4.4 Initialization of Stator and Rotor Currents | 30 |
| | |
| 5. TRANSIENT SOLUTION | 33 |
| 5.1 Introduction | 33 |
| 5.2 The Electrical Equations | 34 |
| 5.3 The Mechanical Equations | 39 |
| 5.4 Saturation in the Leakage Path | 41 |

| | |
|---|-----------|
| 6. OPTIMIZATION ALGORITHM FOR FINDING THE BEST PIECEWISE LINEAR λ - i CHARACTERISTIC | 44 |
| 6.1 Introduction | 44 |
| 6.2 Objective Function | 44 |
| 6.3 Method for Finding the Optimal Solution | 47 |
| 6.4 Examples | 51 |
| 7. CASE STUDY | 54 |
| 8. CONCLUSIONS | 62 |
| REFERENCES | 64 |
| APPENDIX A | 65 |

LIST OF TABLES

| | | |
|------------------|---|----|
| Table 4.1 | Machine Data | 22 |
| Table 4.2 | Machine Parameters of the Motor Network | 28 |
| Table 4.3 | Transmission Line Data | 28 |
| Table 4.4 | Transformer Data | 28 |
| Table 4.5 | Operating Slips Obtained by Using the Compensation Based Method | 29 |
| Table 7.1 | Specifications of the 11 000 HP Induction Motor | 54 |

LIST OF FIGURES

| | | |
|-------------------|--|----|
| Figure 2.1 | Direct Axis Equivalent Circuit of a Synchronous Machine | 4 |
| Figure 2.2 | Equivalent Circuit of a Double-Cage Induction Motor | 5 |
| Figure 3.1 | Simplified Equivalent Circuit of a Double-Cage Induction Motor | 8 |
| Figure 3.2 | Variation of Leakage Reactance with Current | 12 |
| Figure 3.3 | Equivalent Circuit of a Double-Cage Induction Motor with Saturable and Unsaturable Leakage Reactances | 14 |
| Figure 3.4 | Variation of T_{\max} with I_{sat} | 17 |
| Figure 3.5 | Variation of T_{\max} with m | 17 |
| Figure 3.6 | Flowchart for the Data Conversion Algorithm | 18 |
| Figure 4.1 | Definitions of the Parameters in Table 4.1 | 22 |
| Figure 4.2 | Motor Network used to Validate the Compensation Based Method | 27 |
| Figure 4.3 | Definitions of the Current Phasors | 31 |
| Figure 5.1 | Saturation Characteristic and its Piecewise Linear Representation | 42 |
| Figure 6.1 | $\lambda - i$ Characteristic and its Piecewise Linear Representation | 45 |
| Figure 6.2 | Comparison of the Saturation Characteristic and its Piecewise Linear Representation ($I_{\text{sat}} = 1.5 \text{ p.u.}$) | 52 |
| Figure 6.3 | Comparison of the Saturation Characteristic and its Piecewise Linear Representation ($I_{\text{sat}} = 3.0 \text{ p.u.}$) | 53 |
| Figure 7.1 | Comparison of the Continuous Saturation Curve and its Piecewise Linear Representation | 56 |
| Figure 7.2 | Simulation Results for an Induction Motor During Start-up | 57 |
| Figure 7.3 | Steady-State Behavior of an Induction Motor | 60 |

ACKNOWLEDGMENT

I would like to express my gratitude to my supervisor Dr. H. W. Dommel for his guidance and advice throughout the course of my research. Also, I would like to thank for his patience in reading the original drafts of this thesis.

I would like to thank my parents for their care, nurture, and support during the many years I have been in school.

I would also like to thank my friends in both the Power and the Communication groups for providing a pleasant working environment during my stay at U.B.C.

Last, but not the least, I like to thank B.C. Hydro and Power Authority and the Natural Sciences and Engineering Research Council of Canada for their financial support in this research project.

CHAPTER 1

INTRODUCTION

The induction motor is the most common motor type used in industry. In some situations, its transient behavior may require detailed analysis. For example, the starting of an induction motor can cause a voltage depression which may significantly reduce the accelerating torque of the motor. The reduction in the accelerating torque can lengthen the starting time of the motor, which may cause an overheating problem, or in severe cases, may fail to accelerate the motor to its rated speed, and cause the motor to draw large currents continuously. This large current could damage the machine windings permanently.

Voltage depression caused by motor starting may also slow down other motors on the same bus. If the voltage drop is severe, these motors will decelerate significantly and may even stall. The decelerating motors, on the other hand, draw more (reactive) current, causing the bus voltage to be reduced further. In extreme situations, a voltage collapse will occur.

Furthermore, due to the advancement in power electronics, induction motors are now commonly used in adjustable-speed drives. These drives can generate harmonic currents and cause voltage distortions. Moreover, these harmonic currents may excite the resonant circuit formed by the supply network. Thus, the analysis of induction motors together with the power electronic circuits becomes important as well.

The above examples show that it may be necessary to analyze the machine performance and its impact on the supply network in detail in certain situations. Computer

simulation programs are best suited for these types of studies. There are special-purpose programs for induction motor studies, which can be used to analyze certain types of motor transients. The Electromagnetic Transients Program (EMTP) can also be used to study induction motor behavior. It has the advantage that it contains detailed models of many other power system components, such as transmission lines, transformers, and thyristors, etc., which may all affect the transient performance of an induction motor.

In this thesis, a method of simulating the induction motor transients using the EMTP synchronous machine model is discussed. One advantage of this approach is that less code is required for the induction motor. This makes program maintenance easier because only one set of code rather than two must be maintained. If the models for a.c. machines are improved, only one set of code has to be modified. This is somewhat similar to the approach taken for the "universal machine" in the DCG/EPRI and ATP versions of the EMTP [1], which can be used for the simulation of induction machines as well as synchronous machines.

The remainder of this thesis is divided into seven chapters. In Chapter 2, the similarity between the synchronous machine and the induction machine models is discussed. Moreover, the method of converting a synchronous machine model into an induction machine model is described. A data conversion algorithm which converts standard motor specifications into equivalent circuit parameters is explained in Chapter 3. In Chapter 4, methods for finding the steady-state solution of networks with induction motors are presented. The details of implementing a transient analysis program for an induction motor using the 4th-order Runge-Kutta solution method are discussed in Chapter 5. In Chapter 6,

an optimization algorithm for finding the best piecewise linear representation of the continuous saturation characteristic is described. Finally, simulation results of a motor start-up and the general conclusions of this thesis are presented in Chapters 7 and 8, respectively.

CHAPTER 2

SIMILARITY BETWEEN THE SYNCHRONOUS MACHINE AND INDUCTION MACHINE MODELS

In the EMTP, the machine equations are solved in the d-q-o reference frame, which is a reference frame attached to the rotor (d = direct axis of rotor, q = quadrature axis of rotor, o = zero sequence). The d-axis equivalent circuit of the synchronous machine model is shown in Figure 2.1.

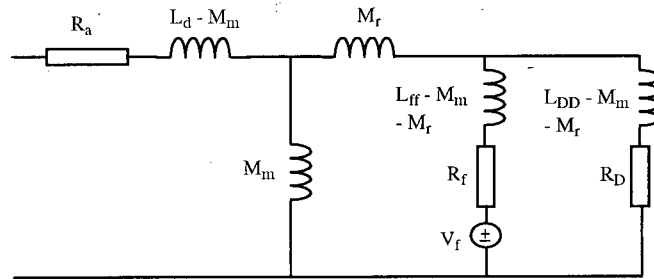


Figure 2.1 Direct Axis Equivalent Circuit of a Synchronous Machine

In Figure 2.1, by setting $V_f = 0$ and replacing subscripts d, f, and D, respectively, with q, g, and Q, the q-axis equivalent circuit is obtained. The D and Q windings are used to represent the damper bar effects, whereas the g-winding is used to model the eddy current effects in a non-salient pole rotor.

The equivalent circuit of a double-cage induction motor is shown in Figure 2.2. Subscripts 1 and 2 are used for the two equivalent circuits on the rotor.

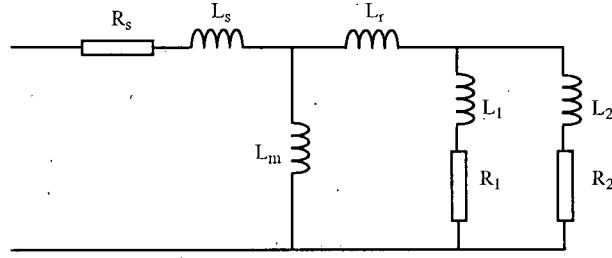


Figure 2.2 Equivalent Circuit of a Double-Cage Induction Motor

Since there is practically no saliency in an induction motor, the equivalent circuit shown in Figure 2.2 is valid for both d- and q- axes. Comparing Figures 2.1 and 2.2, it can be seen that the synchronous machine model is almost identical with that of the induction motor model. In fact, if the field winding of the synchronous machine model is short-circuited, the synchronous machine model will become the induction motor model. The flux and current relationships for both machine types are of the same form. For the synchronous machine, the relationship is

$$\begin{bmatrix} \lambda_d \\ \lambda_f \\ \lambda_D \end{bmatrix} = \begin{bmatrix} L_d & M_{df} & M_{dD} \\ M_{df} & L_{ff} & M_{fD} \\ M_{dD} & M_{fD} & L_{DD} \end{bmatrix} \begin{bmatrix} i_d \\ i_f \\ i_D \end{bmatrix} \quad (2.1)$$

and for the induction machine, it is

$$\begin{bmatrix} \lambda_s \\ \lambda_1 \\ \lambda_2 \end{bmatrix} = \begin{bmatrix} L_s + L_m & L_m & L_m \\ L_m & L_1 + L_r + L_m & L_r + L_m \\ L_m & L_r + L_m & L_2 + L_r + L_m \end{bmatrix} \begin{bmatrix} i_s \\ i_1 \\ i_2 \end{bmatrix} \quad (2.2)$$

From Equations (2.1) and (2.2), the two sets of machine inductances can be related as follows:

$$L_d = L_s + L_m \quad (2.3)$$

$$L_{ff} = L_1 + L_r + L_m \quad (2.4)$$

$$L_{DD} = L_2 + L_r + L_m \quad (2.5)$$

$$M_{fD} = L_r + L_m \quad (2.6)$$

$$M_{df} = M_{dD} = L_m \quad (2.7)$$

Since the induction machine parameters are identical for both d- and q- axes, the q-axis parameters can be obtained by replacing subscripts d, f, and D, respectively, with q, g, and Q in Equations (2.3) - (2.7). The conversions with Equations (2.3) - (2.7), together with setting $V_f = 0$, convert the synchronous machine model into an induction machine model.

CHAPTER 3

DATA CONVERSION

3.1 INTRODUCTION

In order to represent an induction motor accurately in the EMTP, a detailed equivalent circuit of the machine is required. This equivalent circuit should be general enough to model a wide variety of motors, such as motors with deep-bar rotors, double-cage rotors and single-cage rotors. It has been shown earlier [2,3] that the equivalent circuit of a double-cage induction motor, as shown in Figure 2.2, is adequate for these purposes. Even though a model with one circuit on the rotor can be used to represent a single-cage motor, the double-cage model is preferred because the second circuit can be used to represent the frequency-dependent eddy current effects.

In many situations, magnetic saturation has negligible effects on the motor's performance [3]. However, there are cases in which saturation effects do play an important role. In Figure 2.2, three inductances can be influenced by magnetic saturation, namely, the mutual inductance (L_m), the stator leakage inductance (L_s), and the mutual rotor inductance (L_r). These inductances have different degrees of saturation depending on the magnitudes of currents flowing through them. For example, during start-up, large inrush currents will flow into the motor, causing L_s and L_r to saturate, but because of the low rotor resistances, very little inrush current will flow through L_m , and hence, L_m will remain unsaturated. In fact, the saturation effects of L_m are insignificant in most types of studies; nonlinear effects are therefore only considered for L_s and L_r . An exception is the analysis of reclosing transients

of capacitor-compensated motors [4,5], where saturation effects in L_m are also important; for such cases, the model discussed here would have to be modified.

If the very small inductance L_1 of the outer cage is neglected, the simplified equivalent circuit of Figure 3.1 is obtained. This equivalent circuit is considered to be adequate for most system studies, and is therefore used as the induction motor model in the data conversion. The EMTP itself accepts L_1 , which happens to be zero with the data conversion scheme presented in this thesis.

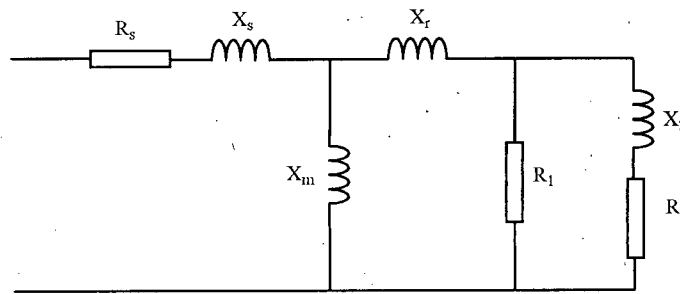


Figure 3.1 Simplified Equivalent Circuit of a Double-Cage Induction Motor

One problem in using this equivalent circuit is that the required parameters may not be known to the user. Even if the manufacturer supplies the user with equivalent circuit parameters, these parameters may not accurately reflect the starting and the full load characteristics of the motor. However, through iterative algorithms, a fairly accurate equivalent circuit can be obtained using the standard motor specifications supplied by the manufacturer. A data conversion algorithm which converts motor specifications into equivalent circuit parameters is therefore developed. Since the manufacturer's data are specified for rated steady-state operating conditions, reactances rather than inductances are used in Figure 3.1 and in the remainder of this chapter.

3.2 CONVERSION ALGORITHM

The data conversion algorithm presented here is based on the work done by Rogers and Shirmohammadi [6], with some modifications. The following data are required as input:

- rated apparent power of the motor or rated (active) power on the shaft
- rated three-phase voltage (line-to-line)
- rated efficiency η
- rated power factor $\cos \theta$
- rated slip s_r
- starting current at rated voltage I_{st} (in p.u.)
- reduced voltage at which another starting current is available, V_{red} (in p.u.)
- starting current at reduced voltage, I_{red} (in p.u.)
- starting torque (in p.u. with respect to full load torque)
- breakdown torque (in p.u. with respect to full load torque)
- saturation threshold current I_{sat} (in p.u.)

In [6], it is suggested that $I_{sat} = 2.0$ p.u. is a good approximation for many induction motors. Hence, I_{sat} has a default value of 2.0 p.u. In the DCG/EPRI version of the EMTP, V_{red} has a default value of 0.8 p.u., whereas I_{red} has a default value of 0.78 times the starting current at rated voltage [1].

Since core loss, friction loss and windage loss are not part of the equivalent circuit, the “effective” efficiency η' must be increased. Assuming that these losses contribute 25% of the total losses in a motor [6], the effective efficiency is

$$\eta' = 0.25 + 0.75 \cdot \eta \quad (3.1)$$

The equivalent circuit parameters may be approximated as follows:

$$R_s = \cos \theta \cdot [1 - \eta' / (1 - s_r)] \quad (3.2)$$

Let R_r be the equivalent rotor resistance. Then

$$R_r = s_r \cdot \eta' / [(1 - s_r) \cdot \cos \theta] \quad (3.3)$$

$$X_m = \eta' / [(1 - s_r) \cdot \sin \theta] \quad (3.4)$$

During start-up, the equivalent rotor resistance R_{st} can be approximated by

$$R_{st} = T_{st} \cdot \eta' \cdot \cos \theta / [(I_{st})^2 \cdot (1 - s_r)] \quad (3.5)$$

where T_{st} is the starting torque and I_{st} is the starting current at rated voltage.

After R_r and R_{st} are determined, the rotor resistances can be calculated as

$$R_1 = R_{st} \cdot (1 + m^2) - R_r \cdot m^2 \quad (3.6)$$

$$R_2 = R_1 \cdot R_r / (R_1 - R_r) \quad (3.7)$$

In Equation (3.6), m is the design ratio. Its normal range is between 0.5 and 1.5 [7]. It is shown in [6] that m is around 1.0 for normal double-cage rotors, and between 0.5 and 0.6 for deep bar rotors. In this conversion procedure, m is initially set to unity and is later adjusted until the breakdown torque requirement is met.

After R_1 and R_2 are determined, X_2 can be calculated as

$$X_2 = (R_1 + R_2) / m \quad (3.8)$$

To take the variation of the leakage reactance into account according to Figure 3.2, the starting currents at two different voltage levels are needed. The total leakage reactance at rated voltage starting (X_{tls}) can be calculated as

$$X_{tls} = \sqrt{\left(\frac{V_s}{I_{st}}\right)^2 - (R_s + R_{st})^2} \quad V_s = 1.0 \text{ p.u.} \quad (3.9)$$

whereas the one at reduced voltage starting (X_{l2}) can be calculated as

$$X_{l2} = \sqrt{\left(\frac{V_{red}}{I_{red}}\right)^2 - (R_s + R_{st})^2} \quad (3.10)$$

The variation of the leakage reactance with current can be represented by a describing function DF [6]:

$$DF = 1.0 \quad \text{for } I \leq I_{sat}$$

$$DF = (2 / \pi) \cdot [\alpha + 0.5 \cdot \sin (2 \cdot \alpha)] \quad \text{for } I > I_{sat}$$

$$\text{where } \alpha = \sin^{-1} (I_{sat} / I) \quad (3.11)$$

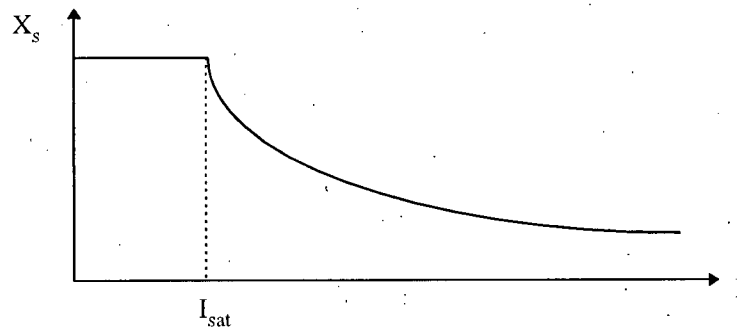


Figure 3.2 Variation of Leakage Reactance with Current

With this function, the total leakage reactance X_l can be expressed as the sum of an unsaturable part X_{t0} and a saturable part X_{ts} , that is,

$$X_{tl} = X_{to} + DF \cdot X_{ts} \quad (3.12)$$

Using Equations (3.9), (3.10), and (3.12), X_{ts} and X_{to} can be calculated as follows:

$$X_{ts} = \frac{(X_{tl2} - X_{tls})}{(DF_2 - DF_s)} \quad (3.13)$$

$$X_{to} = \frac{X_{tls} \cdot DF_2 - X_{tl2} \cdot DF_s}{DF_2 - DF_s} \quad (3.14)$$

where DF_s and DF_2 are obtained from Equation (3.11) using I_{st} and I_{red} , respectively.

If the total saturable and unsaturable leakage reactances are divided equally between the stator and rotor, the reactances can be formulated as follows:

$$X_{so} = X_{to} / 2 \quad (3.15)$$

$$X_{ro} = X_{so} - R_r \cdot (R_1 / R_2) \cdot m / (m^2 + 1) \quad (3.16)$$

$$X_{ss} = X_{ts} / 2 \quad (3.17)$$

$$X_{rs} = X_{ts} / 2 \quad (3.18)$$

At this stage, initial estimates for all circuit parameters are found. Furthermore, both X_s and X_r in Figure 3.1 now consist of two parts, namely, the saturable and the unsaturable parts as shown in Figure 3.3.

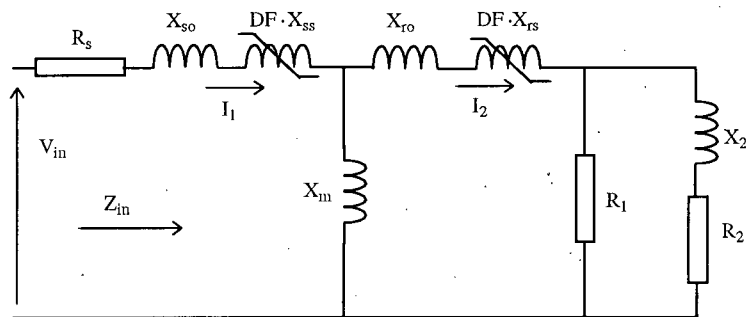


Figure 3.3 Equivalent Circuit of a Double-Cage Induction Motor with Saturable and Unsaturable Leakage Reactances

The accuracy of X_m can be improved to match the manufacturer's data more closely, by using an iterative method involving the power factor [6]. In this method, the induction motor is represented by a transient Thevenin equivalent circuit, which consists of a transient voltage source $V' = V'_d + j V'_q$ behind a transient impedance $Z'_s = R_s + j X'_s$. It can be shown that

$$X'_s = X_{su} \cdot [1 + X_m / (X_m + X_{su})] \quad (3.19)$$

$$V' = (1 - R_s \cdot \cos \theta - X'_s \cdot \sin \theta) + j (-X'_s \cdot \cos \theta + R_s \cdot \sin \theta) \quad (3.20)$$

where X_{su} is the unsaturated leakage reactance of the stator ($X_{su} = X_{so} + X_{ss}$). Using Equation (3.20), the ratio of the imaginary to real parts of V' is

$$\frac{V'_q}{V'_d} = \frac{-X'_s \cdot \cos \theta + R_s \cdot \sin \theta}{1 - R_s \cdot \cos \theta - X'_s \cdot \sin \theta} \quad (3.21)$$

Moreover, a new variable X_s is defined as

$$X_s = \frac{(R_r / s_r) \cdot (\cos \theta - R_s)}{\sin \theta - X'_s} \quad (3.22)$$

where $X_s = X_m + X_{su}$.

After X'_s , $\frac{V'_q}{V_d}$, and X_s are determined, new estimates for R_r and X_m are:

$$R_r = \frac{s_r \cdot X_s \cdot (R_s \cdot \frac{V'_q}{V_d} + X'_s)}{R_s - X_s \cdot \frac{V'_q}{V_d}} \quad (3.23)$$

$$X_m = \sqrt{X_s \cdot (X_s - X'_s)} \quad (3.24)$$

The new values of R_r and X_m are then compared to the old ones. If the differences are larger than an acceptable tolerance, parameters R_1 , R_2 , X_2 , X_{r0} , X'_s , $\frac{V'_q}{V_d}$, X_s , R_r , and X_m are recalculated. Typically, 5 steps are needed for these iterative improvements.

Referring to Figure 3.3, the per-unit torque at slip s is

$$T = (\text{Re}(V_{in} \cdot I_1^*) - |I_1|^2 \cdot R_s) / T_{rate} \quad (3.25)$$

where T_{rate} is the rated machine torque, defined as follow:

$$T_{rate} = \eta' \cdot \cos \theta / (1 - s_r) \quad (3.26)$$

Care must be exercised in determining I_1 used in Equation (3.25). Initially $|I_1|$ and $|I_2|$ are predicted so that the DF(s) for both X_{ss} and X_{rs} can be approximated. After the DF(s) have been estimated, the input impedance Z_{in} can be determined, which, in turn, leads to new values of $|I_1|$ and $|I_2|$. I_1 and I_2 are iterated in this manner until the changes become negligibly small. After I_1 has been determined in this way, the torque at slip s can then be calculated using Equation (3.25).

The breakdown torque for this set of machine parameters is then determined. This actual breakdown torque is compared to the rated breakdown torque. If there is a disagreement, the design ratio m is adjusted [7] and parameters R_1 , R_2 , X_2 , and X_{ro} are recalculated. This process is repeated until the actual and rated breakdown torques are reasonably close.

In [6], the breakdown torque requirement is met by adjusting the saturation threshold current I_{sat} . However, the breakdown torque value is fairly insensitive to changes in I_{sat} , as shown in Figure 3.4. Thus, after the circuit parameters are calculated to satisfy the starting and the full load characteristics, the breakdown torque value can only be adjusted slightly. As a result, the breakdown torque requirement cannot always be met using this approach. The breakdown torque value is very sensitive to changes in m , however, as shown in Figure 3.5. Modifying m is therefore an effective way of meeting the breakdown torque requirement. Moreover, since m is usually unavailable from the manufacturer, it is better to determine it using the rated breakdown torque, rather than assigning a typical value to it.

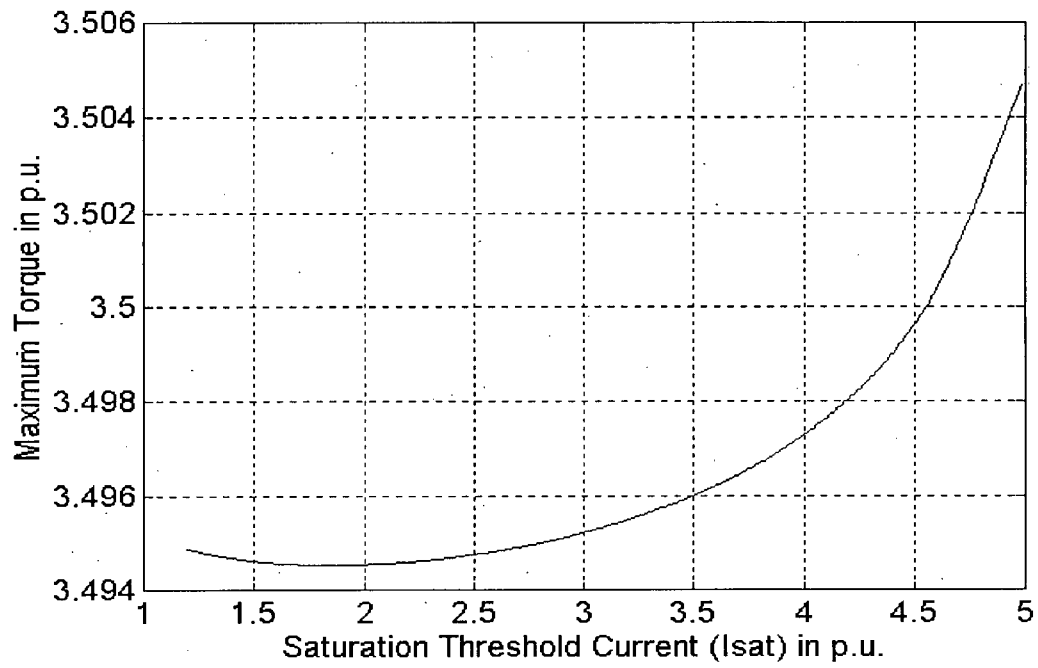


Figure 3.4 Variation of T_{max} with I_{sat}

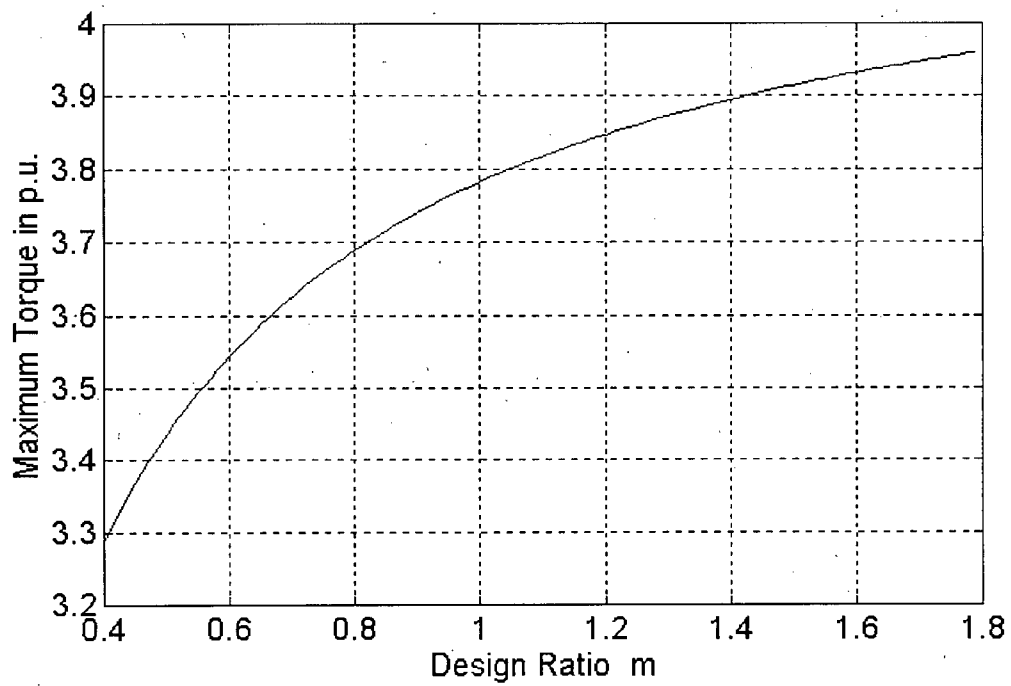


Figure 3.5 Variation of T_{max} with m

To conclude this chapter, the data conversion algorithm is summarized in a flowchart shown in Figure 3.6.

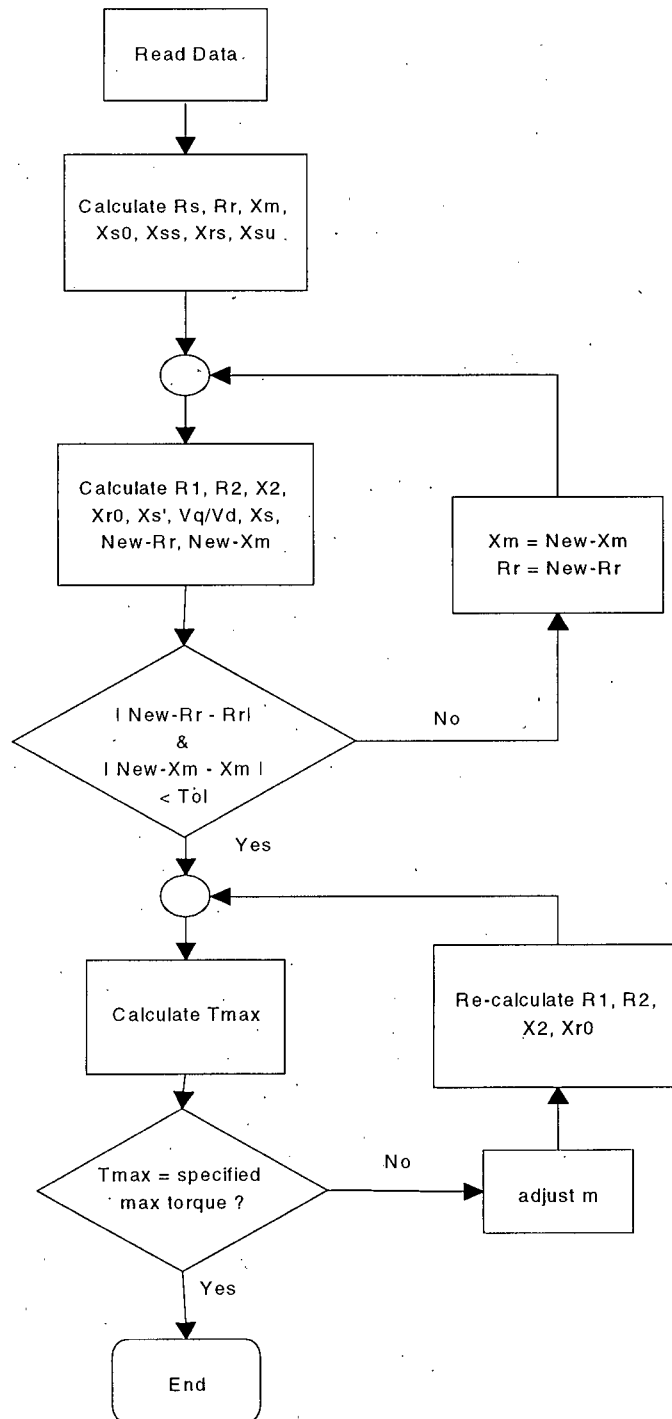


Figure 3.6. Flowchart for the Data Conversion Algorithm

CHAPTER 4

STEADY-STATE REPRESENTATION AND INITIALIZATION

4.1 INTRODUCTION

For balanced steady-state operation, the three-phase induction motor can be represented as three identical impedances Z_{pos} in the three phases. There are several methods for obtaining Z_{pos} , but they all require that the operating slip s_0 be known a priori. The operating slip s_0 will be different from the rated slip, however, if the actual and rated terminal voltages are noticeably different.

One way to obtain Z_{pos} is to find the input impedance of the equivalent circuit in Figure 3.3. Saturation of the leakage reactances can be neglected, since the current will be close to its rated value under steady-state conditions. Another method of finding Z_{pos} is to use the following equation [8]:

$$Z_{\text{pos}} = R_s + j \omega_s L_{aa} - j \omega_s [L_{ar}] \{ [R_r] + j s_0 \omega_s [L_{rr}] \}^{-1} j s_0 \omega_s [L_{ra}] \quad (4.1)$$

where ω_s is the synchronous speed of the supply network and

$$\begin{aligned} L_{aa} &= L_s + L_m, & [L_{ra}] &= \begin{bmatrix} L_m \\ L_m \end{bmatrix}, \\ [L_{ar}] &= \begin{bmatrix} L_m & L_m \end{bmatrix}, & [R_r] &= \begin{bmatrix} R_1 & 0 \\ 0 & R_2 \end{bmatrix}, \\ [L_{rr}] &= \begin{bmatrix} L_1 + L_r + L_m & L_m + L_r \\ L_m + L_r & L_2 + L_r + L_m \end{bmatrix}. \end{aligned} \quad (4.2)$$

In practice, s_0 is not known unless the motor is started from rest ($s_0 = 1$, speed = 0), but it can be found iteratively with a given torque-speed characteristic of the load.

In steady state, the motor is running at a constant speed. The net torque acting on the rotor is therefore zero,

$$T_{\text{motor}} - T_{\text{load}} = 0 \quad (4.3)$$

Since both T_{motor} and T_{load} are functions of slip, Equation (4.3) can be used to find the operating slip s_0 . T_{load} will be known as a function of speed or slip, but the machine torque-slip characteristic $T_{\text{motor}}(s)$ is strongly influenced by the machine terminal voltage, which in turn depends on Z_{pos} and s_0 . Hence, iterative algorithms must be used to find s_0 . In this section, two methods of finding s_0 will be discussed, namely, the Thevenin equivalent based method and the compensation based method.

4.2 THE THEVENIN EQUIVALENT BASED METHOD

In the Thevenin equivalent based method, the network to which the machines are connected, is represented by a Thevenin equivalent circuit. The operating slips of the machines are then determined iteratively using this equivalent circuit. The advantage of this method is that it can be implemented easily as a separated routine, thus, very minor modifications are needed in the existing EMTP code. This method, however, works well only in the cases where the motors are connected to the same bus. In spite of this limitation, this method is quite useful in obtaining the operating slip(s) in single motor analysis and in

motor-starting studies (i.e., the study of the influence of motor starting on other motors on the same bus). This solution method is summarized as follows:

- 1) Obtain the positive sequence Thevenin equivalent circuit of the network to which the motors are connected.
- 2) Set $s_o^{(0)} = s_{rate}$ for each motor.
- 3) Calculate the input impedance Z_{pos} for each motor.
- 4) Calculate the bus voltage, using the voltage divider equation.
- 5) Find the operating slip $s_o^{(i)}$ for each motor with the voltage obtained from step 4, by solving Equation (4.3) with Newton's method.
- 6) Check whether $|s_o^{(i)} - s_o^{(i-1)}|$ is less than a given tolerance for each motor. If yes, stop.
- 7) Otherwise, assign $s_o^{(i)} = s_o^{(i-1)}$ for each motor and go to step 3.

A program was written to validate this solution method. This program contains four sets of machine data and allows the user to obtain the operating slip of each machine. The user is required to enter the number of machines on the bus and the Thevenin voltage and impedance of the supply network. The machine data and their definitions are provided, respectively, in Table 4.1 and Figure 4.1.

Table 4.1 Machine Data [11]

| | Motor #1 | Motor #2 | Motor #3 | Motor #4 |
|----------------------|---------------------|-----------------------------------|---------------------|------------------------|
| R₁ | 0.07 Ω | 0.25 Ω | 0.191 Ω | 0.076 Ω |
| R₂ | 0.05 Ω | 0.2 Ω | 0.0707 Ω | 0.062 Ω |
| X₁ | 0.2 Ω | 1.2 Ω | 0.75398 Ω | 0.195 Ω |
| X₂ | 0.2 Ω | 1.1 Ω | 0.75398 Ω | 0.195 Ω |
| X_m | 6.5 Ω | 35.0 Ω | 16.8892 Ω | 6.386 Ω |
| # of Poles | 8 | 4 | 6 | 8 |
| Rated Slip | 0.04 | 0.02222 | 0.016667 | 0.03 |
| Load Torque | $T = 15.467 \omega$ | $T = 3.08 \cdot 10^{-3} \omega^2$ | $T = 2.4415 \omega$ | $T = 0.11073 \omega^2$ |

Note: rated line-to-line voltage = 460 V

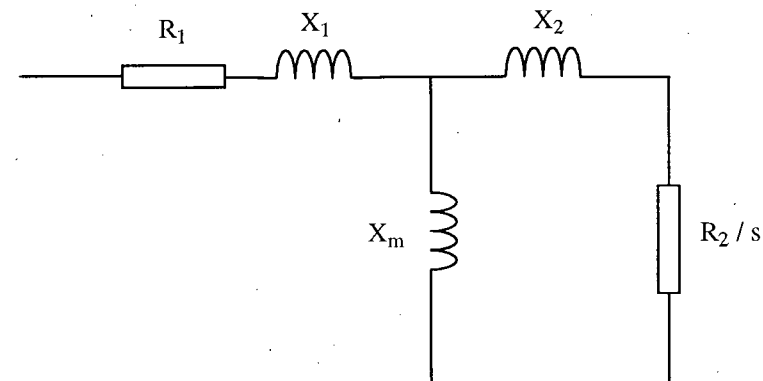


Figure 4.1 Definitions of the Parameters in Table 4.1

Four cases have been studied using this program; the results are summarized as follows:

Case #1

$$R_{th} = 0.0 \, \Omega, X_{th} = 0.0 \, \Omega$$

Number of machines studied: 4

Number of iterations required: 1

Operating slip of motor #1: 0.040000

Operating slip of motor #2: 0.022220

Operating slip of motor #3: 0.016667

Operating slip of motor #4: 0.030000

Net torque on motor #1: 0.00450378 N · m

Net torque on motor #2: -0.00006898 N · m

Net torque on motor #3: -0.00208136 N · m

Net torque on motor #4: 0.00085635 N · m

Case #2

$$R_{th} = 0.0 \, \Omega, X_{th} = 0.02 \, \Omega$$

Number of machines studied: 2

Number of iterations required: 3

Operating slip of motor #1: 0.040814

Operating slip of motor #2: 0.022620

Net torque on motor #1: 0.00837990 N · m

Net torque on motor #2: 0.00062572 N · m

Case #3

$$R_{th} = 0.0 \, \Omega, X_{th} = 0.02 \, \Omega$$

Number of machines studied: 4

Number of iterations required: 4

Operating slip of motor #1: 0.041580

Operating slip of motor #2: 0.022993

Operating slip of motor #3: 0.017363

Operating slip of motor #4: 0.030986

Net torque on motor #1: 0.00149221 N · m

Net torque on motor #2: 0.00010812 N · m

Net torque on motor #3: 0.00029827 N · m

Net torque on motor #4: 0.00098647 N · m

Case #4

$$R_{th} = 0.0 \, \Omega, X_{th} = 0.06 \, \Omega$$

Number of machines studied: 4

Number of iterations required: 6

Operating slip of motor #1: 0.045712

Operating slip of motor #2: 0.024970

Operating slip of motor #3: 0.019215

Operating slip of motor #4: 0.033478

Net torque on motor #1: 0.00346631 N · m

Net torque on motor #2: 0.00025674 N · m

Net torque on motor #3: 0.00073395 N · m

Net torque on motor #4: 0.00227984 N · m

In Case #1, since $R_{th} = X_{th} = 0.0$, the rated voltage is directly applied to the machines; hence, the machines are operating at their rated slips, and the program terminated in one iteration. The situations in Cases #2 and #3 are identical except for the number of

machines involved. It is observed that the number of iterations increases with the number of machines being studied; the increase is minor, however. Case #4 shows that this solution method converges to a correct solution even if a large Thevenin reactance is used. All these results suggest that the Thevenin equivalent based method is an efficient way to obtain the operating slips of motors connected to the same bus.

4.3 THE COMPENSATION BASED METHOD

The operating slips of induction motors can also be obtained using the compensation based method. The advantage of this method is that it can be used to determine the operating slips of motors at different locations; however, its implementation requires more changes in the existing EMTP code, compared to the Thevenin equivalent based method.

The steady-state solution in the EMTP is based on solving the linear nodal equations

$$[Y] \cdot [V] = [I] \quad (4.4)$$

This solution can be modified for steady-state initialization of networks with induction motors as follows:

- 1) Build the admittance matrix $[Y]$ with Z_{pos} , assuming that all induction motors are operating at their rated slips, or $s_o^{(0)} = s_{rate}$ for each motor.
- 2) Triangularize the admittance matrix $[Y]$.

3) Find the voltages at each node by solving Equation (4.4) with downward operations and backward substitutions, using the elements of the triangularized admittance matrix.

4) Find the operating slip $s_o^{(i)}$ for each motor with the voltages from step 3, by solving Equation (4.3) with Newton's method.

5) Check whether $|s_o^{(i)} - s_o^{(i-1)}|$ is less than a given tolerance for each motor.

If yes, stop.

6) Otherwise, add a correction term $I_{\text{corr}(k)}$ to the k^{th} element of the current vector $[I]$

if the slip is not accurate enough for the motor at node k ,

where

$$I_{\text{corr}(k)} = [Y_{\text{pos}_k}(s_{\text{rate}}) - Y_{\text{pos}_k}(s_o^{(i)})] \cdot V_k^{(i)}$$

$$V_k^{(i)} = \text{voltage at node } k \text{ (at } i^{\text{th}} \text{ iteration)}$$

$$Y_{\text{pos}_k}(s_{\text{rate}}) = \text{input admittance of the motor at node } k \text{ at slip } s_{\text{rate}}$$

$$Y_{\text{pos}_k}(s_o^{(i)}) = \text{input admittance of the motor at node } k \text{ at slip } s_o^{(i)}.$$

7) Assign $s_o^{(i-1)} = s_o^{(i)}$ for each motor. Go to step 3.

In step 6, the correction term to the k^{th} element of $[I]$ compensates for the fact that the motor at node k is not operating at its rated slip. One can achieve the same effect by actually updating the $[Y]$ matrix; this method, however, requires re-triangularization of $[Y]$ in each iterative step, while the algorithm described here requires only one triangularization of $[Y]$. Only forward operations and backward substitutions have to be performed in re-

calculating the voltage vector in each iterative step. For one induction motor, the solution usually converged within 2-3 iterations. For more induction motors, the number of iterations may increase.

In order to validate this solution method, a practical motor network is studied [9]. This network consists of five interconnected motors, as shown in Figure 4.2. The machine parameters and the relevant data of the network are provided in Tables 4.2, 4.3, and 4.4.

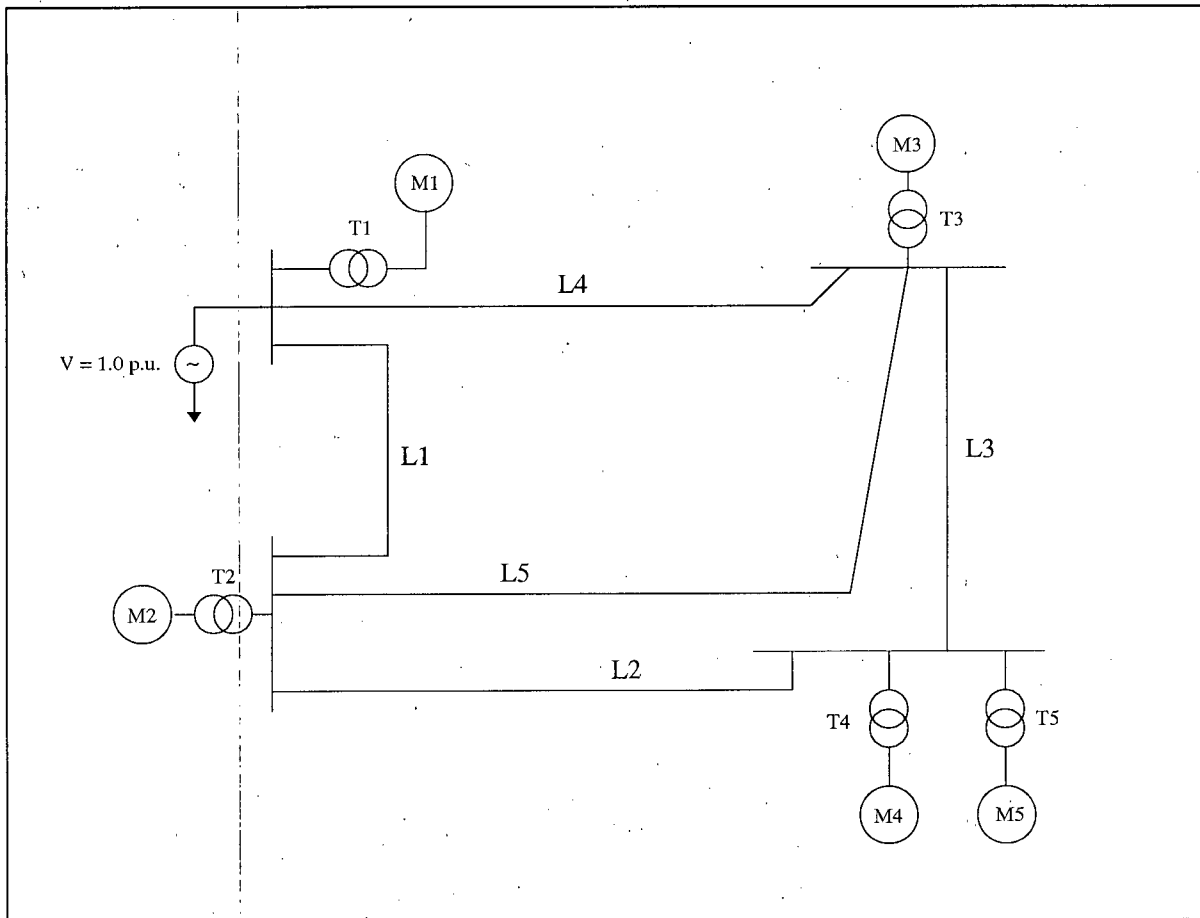


Figure 4.2 Motor Network used to Validate the Compensation Based Method

Table 4.2 Machine Parameters of the Motor Network*Based on 345 kV, 100 MVA*

| | M1, M3, M4 | M2, M5 |
|--|------------|------------|
| S_{rate} | 0.0179 | 0.0083 |
| R₂ | 0.408 p.u. | 0.633 p.u. |
| R₁ | 0.204 p.u. | 2.25 p.u. |
| X₁, X₂ | 2.01 p.u. | 7.0 p.u. |
| X_m | 50.0 p.u. | 157.5 p.u. |
| # of Poles | 2 | 6 |
| Load Torque for M1: $T = 100 + 27.48737 \omega$ Load Torque for M2: $T = 750 + 78.44743 \omega$ Load Torque for M3: $T = 7.49709 \cdot 10^{-2} \omega^2$ Load Torque for M4: $T = 1250 + 6.58522 \cdot 10^{-2} \omega$ Load Torque for M5: $T = 0.677782 \omega^2$ | | |

Refer to Figure 4.1 for definitions of the parameters.

Table 4.3 Transmission Line Data*Based on 345 kV, 100 MVA*

| | Series Resistance | Series Reactance | Shunt Admittance |
|-------------------|-------------------|------------------|------------------|
| Line 1 - 4 | 0.001 p.u. | 0.0055 p.u. | 0.0008 p.u. |
| Line 5 | 0.002 p.u. | 0.0110 p.u. | 0.0016 p.u. |

Table 4.4 Transformer Data*Based on 345 kV, 100 MVA*

| | Transformer Reactance |
|-----------------------------|-----------------------|
| Transformers 1, 3, 4 | 0.3773 p.u. |
| Transformers 2, 5 | 1.2799 p.u. |

Note : The transformer reactances are assumed to be 45% of the corresponding machine rating.

A program was written to determine the operating slips of these machines using the compensation based method. The results of this program are provided in Table 4.5. In order to test the convergence of this iterative algorithm, the transformer reactances are increased to 2.5 times their nominal values. It is observed that an extra iteration is needed to obtain the operating slips after the transformer reactances have been increased. These results indicate that the compensation based method is efficient and robust.

Table 4.5 Operating Slips Obtained by Using the Compensation Based Method

| | Rated Slip | Operating Slip <i>nominal transformer reactance</i> | Operating Slip <i>2.5 times nominal transformer reactance</i> |
|--|-------------------|---|---|
| Motor #1 | 0.017900 | 0.01827689 | 0.01888605 |
| Motor #2 | 0.008300 | 0.01045600 | 0.01091092 |
| Motor #3 | 0.017900 | 0.01827924 | 0.01887615 |
| Motor #4 | 0.017900 | 0.01828497 | 0.01888536 |
| Motor #5 | 0.008300 | 0.01043090 | 0.01087720 |
| Number of iterations for the case of nominal transformer reactance: 3 Number of iterations for the case of 2.5 times nominal transformer reactance: 4 | | | |

4.4 INITIALIZATION OF STATOR AND ROTOR CURRENTS

After the operating slip s_0 is determined, the stator currents in phases a, b, and c can be calculated. Suppose that the stator currents are as follows:

$$\begin{aligned}i_a(t) &= |I| \cos(\omega_s t + \alpha) \\i_b(t) &= |I| \cos(\omega_s t + \alpha - 120^\circ) \\i_c(t) &= |I| \cos(\omega_s t + \alpha - 240^\circ)\end{aligned}\tag{4.5}$$

Then, the corresponding currents in the d,q,o- reference frame are

$$\begin{aligned}i_d(t) &= \sqrt{\frac{3}{2}} |I| \sin(s_0 \omega_s t + \alpha - \delta) \\i_q(t) &= \sqrt{\frac{3}{2}} |I| \cos(s_0 \omega_s t + \alpha - \delta) \\i_o(t) &= 0\end{aligned}\tag{4.6}$$

where δ is the angle between the position of the quadrature axis and the real axis. For induction motors, δ can be set to any arbitrary value. After δ is chosen, initial value for β can be determined as follows:

$$\beta(0) = \delta + \frac{\pi}{2}\tag{4.7}$$

The d- and q- axis stator currents can be represented by a complex phasor

$$\bar{I}_{dq} = \sqrt{\frac{3}{2}} |I| e^{j(\alpha - \delta)} \quad (4.8)$$

with the understanding that

$$\begin{aligned} i_q(t) &= \text{Re} \{ \bar{I}_{dq} e^{js_o \omega_s t} \} \\ i_d(t) &= \text{Im} \{ \bar{I}_{dq} e^{js_o \omega_s t} \} \end{aligned} \quad (4.9)$$

As can be seen from Figure 4.3, the current phasors \bar{I}_{r1dq} and \bar{I}_{r2dq} can be calculated using current division techniques after \bar{I}_{dq} has been determined. The real and imaginary parts of these phasors, respectively, represent the corresponding q- and d- axis rotor currents.

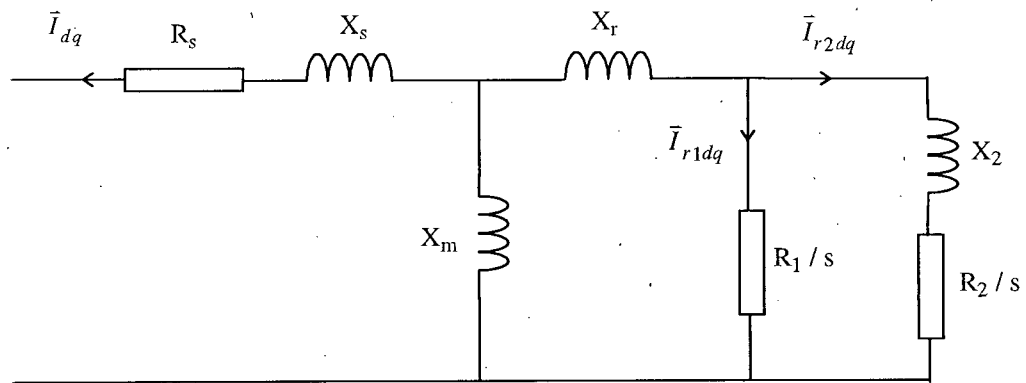


Figure 4.3 Definitions of the Current Phasors

Another way to obtain the current phasors \tilde{I}_{r1dq} and \tilde{I}_{r2dq} is to use the following equation [8] :

$$\begin{bmatrix} \tilde{I}_{r1dq} \\ \tilde{I}_{r2dq} \end{bmatrix} = -\{[R_r] + j s_o \omega_s [L_{rr}]\}^{-1} j s_o \omega_s [L_{ra}] \tilde{I}_{dq} \quad (4.10)$$

where $[R_r]$, $[L_{rr}]$ and $[L_{ra}]$ are defined in Equation (4.2).

In summary, the steady-state solution of an induction machine consists of two parts: determination of the operating slip and initialization of the machine currents. The operating slip is determined using either the Thevenin equivalent based method or the compensation based method. After the operating slip is found, the stator currents can be determined. These currents are then used to calculate the rotor currents using either the current division techniques or Equation (4.10).

CHAPTER 5

TRANSIENT SOLUTION

5.1 INTRODUCTION

The minor modifications in the synchronous machine model to make it behave as an induction motor model have been implemented in UBC's EMTP version MicroTran®. The actual program changes were minor [10] and were done by Dr. H. W. Dommel because he knows the details of the EMTP code better. In order to validate the EMTP results, an independent simulation program, based on the 4th-order Runge-Kutta solution method, was written. The purpose of this program is to study the induction motor behavior during start-up. The supply network is represented by a Thevenin equivalent circuit, i.e., a voltage source, V , behind a positive sequence inductance, L_{ext} .

The behavior of an induction machine is governed by two sets of equations, namely, the electrical equations and the mechanical equations. These two sets of equations are not independent from each other; in fact, they are closely related to each other through the following three variables: speed, angle position, and the net torque acting on the rotor. In this chapter, the details of solving these two sets of equations using the 4th-order Runge-Kutta method will be discussed.

5.2. THE ELECTRICAL EQUATIONS

The voltage and current relationships of an induction motor are governed by the following voltage equations:

$$[v_{abc}] = -[R][i_{abc}] - \frac{d}{dt}[\lambda_{abc}] \quad (5.1)$$

where $[v] = [v_a, v_b, v_c, v_f, v_g, v_D, v_Q]^T$

$$[i] = [i_a, i_b, i_c, i_f, i_g, i_D, i_Q]^T$$

$$[\lambda] = [\lambda_a, \lambda_b, \lambda_c, \lambda_f, \lambda_g, \lambda_D, \lambda_Q]^T$$

$$[R] = \text{diag} [R_a, R_a, R_a, R_f, R_g, R_D, R_Q] \text{ (subscript 'a' for armature).}$$

The generator convention is used in Equation (5.1), i.e., positive currents are going out from the machine terminals.

In order to simplify the calculations, the voltage equations are solved in the d-q-o reference frame, which is a reference frame attached to the rotor. The phase quantities are transformed to d-q-o quantities through the transformation matrix $[T]^{-1}$. That is,

$$[v_{dqo}] = [T]^{-1} [v_{abc}]$$

$$[i_{dqo}] = [T]^{-1} [i_{abc}]$$

$$[\lambda_{dqo}] = [T]^{-1} [\lambda_{abc}] \quad (5.2)$$

where

$$[T]^{-1} = \sqrt{\frac{2}{3}} \begin{bmatrix} \cos \beta & \cos(\beta - 120^\circ) & \cos(\beta + 120^\circ) & 0 & 0 & 0 & 0 \\ \sin \beta & \sin(\beta - 120^\circ) & \sin(\beta + 120^\circ) & 0 & 0 & 0 & 0 \\ \frac{1}{\sqrt{2}} & \frac{1}{\sqrt{2}} & \frac{1}{\sqrt{2}} & 0 & 0 & 0 & 0 \\ 0 & 0 & 0 & 1 & 0 & 0 & 0 \\ 0 & 0 & 0 & 0 & 1 & 0 & 0 \\ 0 & 0 & 0 & 0 & 0 & 1 & 0 \\ 0 & 0 & 0 & 0 & 0 & 0 & 1 \end{bmatrix} \quad (5.3)$$

and where β is the angular position of the rotor relative to the stator, measured in electrical radians.

In this transformation, the stator variables in phase quantities are projected onto the rotating reference frame, while the rotor variables are unaffected. Moreover, this transformation matrix is orthogonal, that is

$$[T] = ([T]^{-1})^T \quad (5.4)$$

To include the inductance of the supply network, an extra term is added to the voltage equations,

$$[v_{abc}] = -[L_{ext}] \frac{d}{dt} [i_{abc}] - [R][i_{abc}] - \frac{d}{dt} [\lambda_{abc}] \quad (5.5)$$

where $[L_{ext}] = \text{diag}[L_{ext}, L_{ext}, L_{ext}, 0, 0, 0, 0]$.

Expressing the a, b, c - quantities as d, q, o- quantities, Equation (5.5) becomes

$$[T] [v_{dqo}] = - [L_{ext}] \frac{d}{dt} \{ [T] [i_{dqo}] \} - [R] [T] [i_{dqo}] - \frac{d}{dt} \{ [T] [\lambda_{dqo}] \} \quad (5.6)$$

$$\begin{aligned} [v_{dqo}] = & - [T]^{-1} [L_{ext}] [T] [T]^{-1} \left\{ \frac{d}{dt} [T] [i_{dqo}] + [T] \frac{d}{dt} [i_{dqo}] \right\} - [T]^{-1} [R] [T] [i_{dqo}] \\ & - [T]^{-1} \left\{ \frac{d}{dt} [T] [\lambda_{dqo}] + [T] \frac{d}{dt} [\lambda_{dqo}] \right\} \end{aligned} \quad (5.7)$$

Since $[T]^{-1} \frac{d}{dt} [T] = [\omega]$, where

$$[\omega] = \begin{bmatrix} 0 & \omega & 0 & 0 & 0 & 0 & 0 \\ -\omega & 0 & 0 & 0 & 0 & 0 & 0 \\ 0 & 0 & 0 & 0 & 0 & 0 & 0 \\ 0 & 0 & 0 & 0 & 0 & 0 & 0 \\ 0 & 0 & 0 & 0 & 0 & 0 & 0 \\ 0 & 0 & 0 & 0 & 0 & 0 & 0 \\ 0 & 0 & 0 & 0 & 0 & 0 & 0 \end{bmatrix} \quad (5.8)$$

and

$$[\lambda_{dqo}] = [L_{dqo}] [i_{dqo}] \quad (5.9)$$

where

$$[L_{dqo}] = \begin{bmatrix} L_d & 0 & 0 & M_{df} & 0 & M_{dD} & 0 \\ 0 & L_q & 0 & 0 & M_{qg} & 0 & M_{qQ} \\ 0 & 0 & L_o & 0 & 0 & 0 & 0 \\ M_{df} & 0 & 0 & L_{ff} & 0 & M_{fD} & 0 \\ 0 & M_{qg} & 0 & 0 & L_{gg} & 0 & M_{gQ} \\ M_{dD} & 0 & 0 & M_{fD} & 0 & L_{DD} & 0 \\ 0 & M_{qQ} & 0 & 0 & M_{gQ} & 0 & L_{QQ} \end{bmatrix} \quad (5.10)$$

with

$$L_d = L_q = L_s + L_m \quad (5.11a)$$

$$L_o = L_s \quad (5.11b)$$

$$L_{ff} = L_{gg} = L_1 + L_r + L_m \quad (5.11c)$$

$$L_{DD} = L_{QQ} = L_2 + L_r + L_m \quad (5.11d)$$

$$M_{fD} = M_{gQ} = L_r + L_m \quad (5.11e)$$

$$M_{df} = M_{dD} = M_{qg} = M_{qQ} = L_m \quad (5.11f)$$

the voltage equations can be expressed as

$$\begin{aligned} [v_{dqo}] = & - [T]^{-1} [L_{ext}] [T] \left\{ [\omega] [i_{dqo}] + \frac{d}{dt} [i_{dqo}] \right\} - [R] [i_{dqo}] \\ & - \left\{ [\omega] [L_{dqo}] [i_{dqo}] + [L_{dqo}] \frac{d}{dt} [i_{dqo}] \right\} \end{aligned} \quad (5.12)$$

Let $[M] = [T]^{-1} \cdot [L_{\text{ext}}] \cdot [T]$.

Then

$$[v_{dqo}] = - \{ [M] [\omega] + [R] + [\omega] [L_{dqo}] \} [i_{dqo}] - \{ [M] + [L_{dqo}] \} \frac{d}{dt} [i_{dqo}] \quad (5.13)$$

Define

$$[A] = [M] [\omega] + [R] + [\omega] [L_{dqo}]$$

and

$$[B] = [M] + [L_{dqo}]$$

then

$$[v_{dqo}] = - [A] [i_{dqo}] - [B] \frac{d}{dt} [i_{dqo}] \quad (5.14)$$

$$\frac{d}{dt} [i_{dqo}] = - [B]^{-1} [A] [i_{dqo}] - [B]^{-1} [v_{dqo}] \quad (5.15)$$

Equation (5.15) is a set of first order ordinary differential equations, which can be solved using 4th-order Runge-Kutta method. In each time step, ω and β must be known in order to evaluate the right-hand side of Equation (5.15). These two variables, however, are not known until the mechanical equations, which also depend on $[i_{dqo}]$, are solved. As a result, at the beginning of each time step, β and ω are first predicted using Equations (5.16) and (5.17), respectively.

$$\beta(t) = \beta(t - \Delta t) + 0.5 \Delta t [\omega(t - \Delta t) + \omega(t)] \quad (5.16)$$

and

$$\omega(t) = 2 \omega(t - \Delta t) - \omega(t - 2\Delta t) \quad (5.17)$$

After $\beta(t)$ and $\omega(t)$ are predicted, $[i_{dqo}(t)]$ is then determined, which, in turn, enables the mechanical equations to be solved. Upon solving the mechanical equations, new values of $\beta(t)$ and $\omega(t)$ are obtained. These values are compared with the ones predicted earlier. If they are reasonably close, the program will proceed to the next time step. Otherwise, $[i_{dqo}(t)]$ are re-calculated using the new values of β and ω .

Alternatively, the mechanical equations [Equations (5.18) and (5.19)], could have been added to the electrical equations [Equation (5.15)] to form a system of nine ordinary differential equations. These equations can then be solved simultaneously without using the prediction formulas. However, the method described here resembles the EMTP solution method more closely, and is therefore used to solve the two sets of differential equations.

5.3 THE MECHANICAL EQUATIONS

The mechanical variables of an induction motor are governed by the following differential equations:

$$J \frac{d\omega}{dt} = T_{net} \quad (5.18)$$

and

$$\frac{d\beta}{dt} = \omega \quad (5.19)$$

where J is the moment of inertia of the rotor and mechanical load, and T_{net} is the net torque acting on it. Using the generator convention, T_{net} is defined as

$$T_{\text{net}} = T_{\text{mech}} - T_{\text{elec}} \quad (5.20)$$

where T_{mech} is the mechanical torque of the mechanical load and T_{elec} is the electrical torque defined as:

$$T_{\text{elec}} = \lambda_d i_q - \lambda_q i_d \quad (5.21)$$

Equations (5.18) and (5.19) can be solved using the trapezoidal integration rule:

$$\omega(t) = \frac{\Delta t}{2J} [T_{\text{net}}(t) + T_{\text{net}}(t - \Delta t)] + \omega(t - \Delta t) \quad (5.22)$$

and

$$\beta(t) = \frac{\Delta t}{2} [\omega(t) + \omega(t - \Delta t)] + \beta(t - \Delta t) \quad (5.23)$$

All the quantities in Equations (5.18) - (5.23) are referred to the electrical side; however, these equations are also valid for mechanical quantities, provided that the following conversions are used:

$$J_{\text{elec}} = J_{\text{mech}} / (P/2)^2 \quad (5.24a)$$

$$\beta_{\text{elec}} = (P/2) \beta_{\text{mech}} \quad (5.24b)$$

$$T_{\text{elec}} = T_{\text{mech}} / (P/2) \quad (5.24c)$$

$$\omega_{\text{elec}} = (P/2) \omega_{\text{mech}} \quad (5.24d)$$

where P is the number of poles.

5.4 SATURATION IN THE LEAKAGE PATH

In the previous equations, saturation effects were ignored. With minor modifications in some of the equations, it is possible to include the leakage saturation effects. Instead of having two nonlinear leakage inductances, as shown in Figure 3.3, the nonlinear inductances L_{ss} and L_{rs} are represented by a single nonlinear inductance L_{sat} outside the machine terminals. In fact, the nonlinear effects of the stator leakage inductance cannot be modeled in the $d,q,0$ - reference frame, since the currents in the d,q - circuits are at slip frequency, which is quite different from the supply frequency in the stator coils. For the rotor leakage inductance, the situation is different, but rotor saturation is usually small compared to stator saturation. Modeling the leakage saturation outside the machine terminals results in the following modifications in $[L_{\text{ext}}]$ and in some elements of $[L_{dq0}]$:

$$[L_{\text{ext}}] = \text{diag}[L_{\text{ext}} + L_{\text{sat}}(i_a), L_{\text{ext}} + L_{\text{sat}}(i_b), L_{\text{ext}} + L_{\text{sat}}(i_c), 0, 0, 0, 0] \quad (5.25)$$

and

$$L_d = L_{so} + L_m$$

$$L_{df} = L_{dD} = L_m$$

$$L_{fD} = L_{ff} = L_{ro} + L_m$$

$$L_{DD} = L_m + L_{ro} + L_2 \quad (5.26)$$

and analogous equations for the q-axis quantities.

The flux and current relationship of L_{sat} is defined as follows:

$$\lambda = (L_{ss} + L_{rs}) \cdot DF(i) \cdot i \quad (5.27)$$

This nonlinear relationship can be represented fairly accurately by a piecewise linear inductance with five slopes, as shown in Figure 5.1.

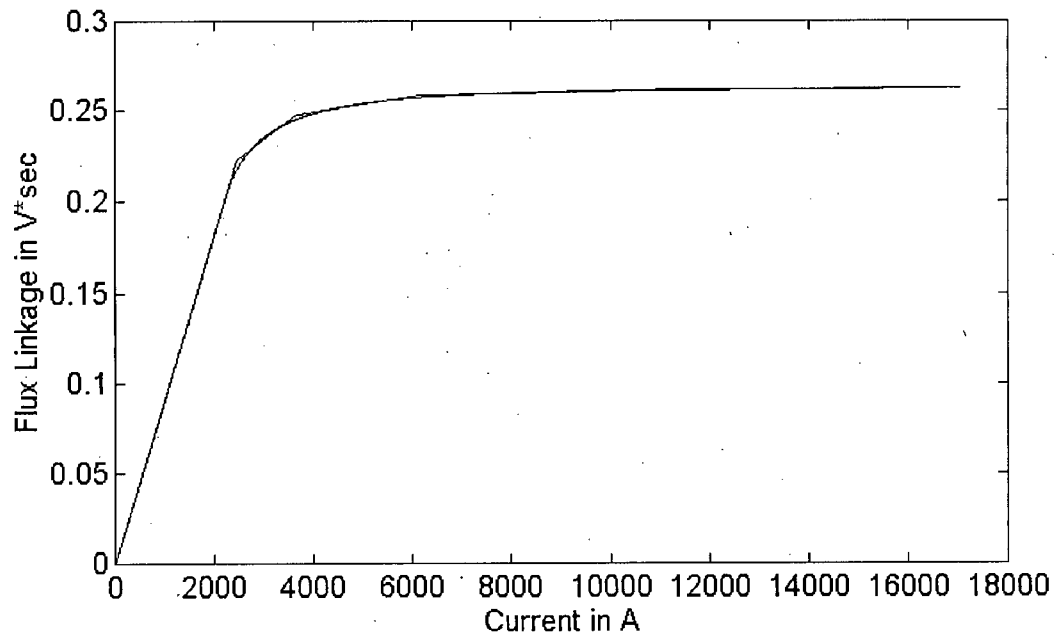


Figure 5.1 Saturation Characteristic and its Piecewise Linear Representation

L_{sat} in each phase may have different values, depending on the magnitude of the phase current flowing through it. In each time step, it is therefore necessary to check whether the phase current is still in the region in which the inductance is valid. If not, the inductance must be adjusted before proceeding to the next time step. This suggests that overshooting problems may occur at change-over points. In order to minimize the overshoot, a small time step Δt should be used. It was found that Δt in the range of 0.1 ms to 0.5 ms is appropriate for this type of transient analysis.

CHAPTER 6

OPTIMIZATION ALGORITHM FOR FINDING THE BEST PIECEWISE LINEAR λ - i CHARACTERISTIC

6.1 INTRODUCTION

In the previous chapter, it was shown that the nonlinear λ - i characteristic can be represented by a piecewise linear inductance with five slopes. In the EMTP, the nonlinear inductances are also represented by piecewise linear segments. In this chapter, an optimization algorithm is discussed for finding a best-fit piecewise linear representation of the λ - i curve

$$\lambda(i) = L \cdot DF(i) \cdot i \quad (6.1)$$

Moreover, two examples are given to illustrate this optimization algorithm.

6.2 OBJECTIVE FUNCTION

A nonlinear λ - i characteristic and its piecewise linear representation with five slopes are shown in Figure 6.1.

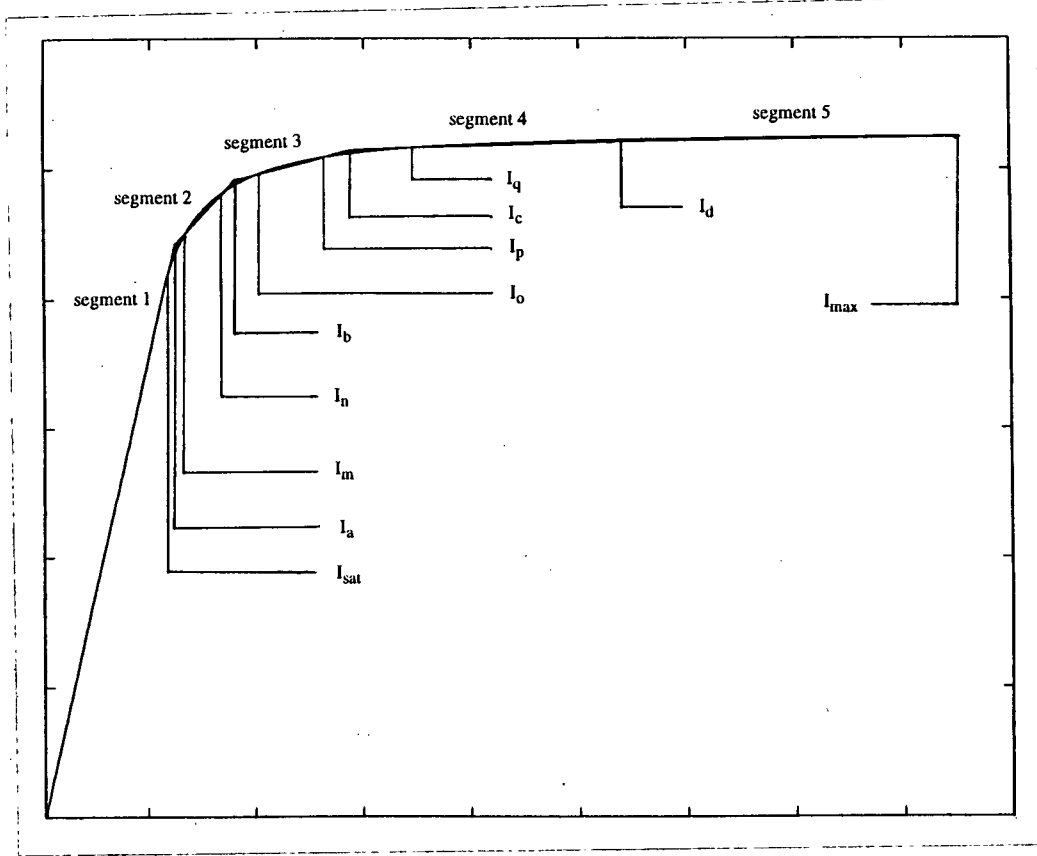


Figure 6.1 $\lambda - i$ Characteristic and its Piecewise Linear Representation

One possible criterion for selecting an optimal piecewise linear characteristic is to minimize the total area between the exact and the fitted curve (Figure 6.1). The equation for each line segment is as follows:

$$\text{segment 1: } \Lambda = L \cdot i \quad (6.2)$$

$$\text{segment 2: } \Lambda = \{ [\lambda(I_n) - \lambda(I_m)] \cdot i + [\lambda(I_m) \cdot I_n - \lambda(I_n) \cdot I_m] \} / [I_n - I_m] \quad (6.3)$$

$$\text{segment 3: } \Lambda = \{ [\lambda(I_p) - \lambda(I_o)] \cdot i + [\lambda(I_o) \cdot I_p - \lambda(I_p) \cdot I_o] \} / [I_p - I_o] \quad (6.4)$$

$$\text{segment 4: } \Lambda = \{ [\lambda(I_d) - \lambda(I_q)] \cdot i + [\lambda(I_q) \cdot I_d - \lambda(I_d) \cdot I_q] \} / [I_d - I_q] \quad (6.5)$$

$$\text{segment 5: } \Lambda = \{ [\lambda(I_{\max}) - \lambda(I_d)] \cdot i + [\lambda(I_d) \cdot I_{\max} - \lambda(I_{\max}) \cdot I_d] \} / [I_{\max} - I_d] \quad (6.6)$$

Define

$$M(I_1, I_2) = \frac{\lambda(I_2) - \lambda(I_1)}{I_2 - I_1} \quad (6.7)$$

and

$$C(I_1, I_2) = \frac{\lambda(I_1) \cdot I_2 - \lambda(I_2) \cdot I_1}{I_2 - I_1} \quad (6.8)$$

Then Equations (6.2) - (6.6) become

$$\text{segment 1:} \quad \Lambda = L \cdot i \quad (6.9)$$

$$\text{segment 2:} \quad \Lambda = M(I_m, I_n) \cdot i + C(I_m, I_n) \quad (6.10)$$

$$\text{segment 3:} \quad \Lambda = M(I_o, I_p) \cdot i + C(I_o, I_p) \quad (6.11)$$

$$\text{segment 4:} \quad \Lambda = M(I_q, I_d) \cdot i + C(I_q, I_d) \quad (6.12)$$

$$\text{segment 5:} \quad \Lambda = M(I_d, I_{\max}) \cdot i + C(I_d, I_{\max}) \quad (6.13)$$

Using Equations (6.9) - (6.13), the total area between the exact and the fitted curves can be formulated as follows:

$$\begin{aligned}
A = & \int_{I_{sat}}^{I_a} [L \cdot i - \lambda(i)] di + \int_{I_a}^{I_m} [M(I_m, I_n) \cdot i + C(I_m, I_n) - \lambda(i)] di \\
& + \int_{I_m}^{I_n} [\lambda(i) - M(I_m, I_n) \cdot i - C(I_m, I_n)] di + \int_{I_n}^{I_b} [M(I_m, I_n) \cdot i + C(I_m, I_n) - \lambda(i)] di \\
& + \int_{I_b}^{I_o} [M(I_o, I_p) \cdot i + C(I_o, I_p) - \lambda(i)] di + \int_{I_o}^{I_p} [\lambda(i) - M(I_o, I_p) \cdot i - C(I_o, I_p)] di \\
& + \int_{I_p}^{I_c} [M(I_o, I_p) \cdot i + C(I_o, I_p) - \lambda(i)] di + \int_{I_c}^{I_q} [M(I_q, I_d) \cdot i + C(I_q, I_d) - \lambda(i)] di \\
& + \int_{I_q}^{I_d} [\lambda(i) - M(I_q, I_d) \cdot i - C(I_q, I_d)] di + \int_{I_d}^{I_{max}} [\lambda(i) - M(I_d, I_{max}) \cdot i - C(I_d, I_{max})] di \quad (6.14)
\end{aligned}$$

The goal of the optimization is to find optimal values for independent variables I_a , I_b , I_c , I_d , I_m , I_n , I_o , I_p , and I_q , such that the objective function A becomes a minimum.

6.3 METHOD FOR FINDING THE OPTIMAL SOLUTION

At the minimum point of A , the partial derivatives of A with respect to all independent variables must be zero. That is,

$$\frac{\partial A}{\partial I_a} = L \cdot I_a - M(I_m, I_n) \cdot I_a - C(I_m, I_n) = 0 \quad (6.15)$$

$$\frac{\partial A}{\partial I_b} = [M(I_m, I_n) - M(I_o, I_p)] \cdot I_b + C(I_m, I_n) - C(I_o, I_p) = 0 \quad (6.16)$$

$$\frac{\partial A}{\partial I_c} = [M(I_o, I_p) - M(I_q, I_d)] \cdot I_c + C(I_o, I_p) - C(I_q, I_d) = 0 \quad (6.17)$$

$$\begin{aligned} \frac{\partial A}{\partial I_d} &= 0.5 \cdot (2 I_q^2 - I_c^2 - I_d^2) \cdot \frac{\partial}{\partial I_d} M(I_q, I_d) + (2 I_q - I_c - I_d) \cdot \frac{\partial}{\partial I_d} C(I_q, I_d) \\ &\quad - I_d \cdot M(I_q, I_d) - C(I_q, I_d) - 0.5 \cdot (I_{\max}^2 - I_d^2) \cdot \frac{\partial}{\partial I_d} M(I_d, I_{\max}) \\ &\quad + I_d \cdot M(I_d, I_{\max}) - (I_{\max} - I_d) \cdot \frac{\partial}{\partial I_d} C(I_d, I_{\max}) + C(I_d, I_{\max}) \\ &= 0 \end{aligned} \quad (6.18)$$

$$\begin{aligned} \frac{\partial A}{\partial I_m} &= 0.5 \cdot (2 I_m^2 - I_a^2 - 2 I_n^2 + I_b^2) \cdot \frac{\partial}{\partial I_m} M(I_m, I_n) + 2 I_m \cdot M(I_m, I_n) \\ &\quad + (2 I_m - I_a - 2 I_n + I_b) \cdot \frac{\partial}{\partial I_m} C(I_m, I_n) + 2 C(I_m, I_n) - 2 \lambda(I_m) \\ &= 0 \end{aligned} \quad (6.19)$$

$$\begin{aligned} \frac{\partial A}{\partial I_n} &= 0.5 \cdot (2 I_m^2 - I_a^2 - 2 I_n^2 + I_b^2) \cdot \frac{\partial}{\partial I_n} M(I_m, I_n) - 2 I_n \cdot M(I_m, I_n) \\ &\quad + (2 I_m - I_a - 2 I_n + I_b) \cdot \frac{\partial}{\partial I_n} C(I_m, I_n) - 2 C(I_m, I_n) + 2 \lambda(I_n) \\ &= 0 \end{aligned} \quad (6.20)$$

$$\begin{aligned}
\frac{\partial A}{\partial I_o} &= 0.5 \cdot (2 I_o^2 - I_b^2 - 2 I_p^2 + I_c^2) \cdot \frac{\partial}{\partial I_o} M(I_o, I_p) + 2 I_o \cdot M(I_o, I_p) \\
&\quad + (2 I_o - I_b - 2 I_p + I_c) \cdot \frac{\partial}{\partial I_o} C(I_o, I_p) + 2 C(I_o, I_p) - 2 \lambda(I_o) \\
&= 0
\end{aligned} \tag{6.21}$$

$$\begin{aligned}
\frac{\partial A}{\partial I_p} &= 0.5 \cdot (2 I_o^2 - I_b^2 - 2 I_p^2 + I_c^2) \cdot \frac{\partial}{\partial I_p} M(I_o, I_p) - 2 I_p \cdot M(I_o, I_p) \\
&\quad + (2 I_o - I_b - 2 I_p + I_c) \cdot \frac{\partial}{\partial I_p} C(I_o, I_p) - 2 C(I_o, I_p) + 2 \lambda(I_p) \\
&= 0
\end{aligned} \tag{6.22}$$

$$\begin{aligned}
\frac{\partial A}{\partial I_q} &= 0.5 \cdot (2 I_q^2 - I_c^2 - I_d^2) \cdot \frac{\partial}{\partial I_q} M(I_q, I_d) + 2 I_q \cdot M(I_q, I_d) \\
&\quad + (2 I_q - I_c - I_d) \cdot \frac{\partial}{\partial I_q} C(I_q, I_d) + 2 C(I_q, I_d) - 2 \lambda(I_q) \\
&= 0
\end{aligned} \tag{6.23}$$

This system of nonlinear equations can be solved with the Newton-Raphson method. The procedure for using this method can be summarized as follows:

- 1) Set $n = 0$.
- 2) Estimate the initial current vector $\mathbf{I}^{(n)} = [I_a, I_b, I_c, I_d, I_m, I_n, I_o, I_p, I_q]^T$
- 3) Evaluate the derivative vector $\mathbf{F}^{(n)}$ using $\mathbf{I}^{(n)}$,

where

$$\mathbf{F}^{(n)} = [F_1, F_2, F_3, F_4, F_5, F_6, F_7, F_8, F_9]^T$$

$$= \left[\begin{array}{ccccccccc} \frac{\partial A}{\partial I_a} & \frac{\partial A}{\partial I_b} & \frac{\partial A}{\partial I_c} & \frac{\partial A}{\partial I_d} & \frac{\partial A}{\partial I_m} & \frac{\partial A}{\partial I_n} & \frac{\partial A}{\partial I_o} & \frac{\partial A}{\partial I_p} & \frac{\partial A}{\partial I_q} \end{array} \right]^T$$

4) Evaluate the Jacobian Matrix $\mathbf{J}^{(n)}$ using $\mathbf{I}^{(n)}$.

where

$$[J] = \left[\begin{array}{ccccccccc} \frac{\partial F_1}{\partial I_a} & 0 & 0 & 0 & \frac{\partial F_1}{\partial I_m} & \frac{\partial F_1}{\partial I_n} & 0 & 0 & 0 \\ 0 & \frac{\partial F_2}{\partial I_b} & 0 & 0 & \frac{\partial F_2}{\partial I_m} & \frac{\partial F_2}{\partial I_n} & \frac{\partial F_2}{\partial I_o} & \frac{\partial F_2}{\partial I_p} & 0 \\ 0 & 0 & \frac{\partial F_3}{\partial I_c} & \frac{\partial F_3}{\partial I_d} & 0 & 0 & \frac{\partial F_3}{\partial I_o} & \frac{\partial F_3}{\partial I_p} & \frac{\partial F_3}{\partial I_q} \\ 0 & 0 & \frac{\partial F_4}{\partial I_c} & \frac{\partial F_4}{\partial I_d} & 0 & 0 & 0 & 0 & \frac{\partial F_4}{\partial I_q} \\ \frac{\partial F_5}{\partial I_a} & \frac{\partial F_5}{\partial I_b} & 0 & 0 & \frac{\partial F_5}{\partial I_m} & \frac{\partial F_5}{\partial I_n} & 0 & 0 & 0 \\ \frac{\partial F_6}{\partial I_a} & \frac{\partial F_6}{\partial I_b} & 0 & 0 & \frac{\partial F_6}{\partial I_m} & \frac{\partial F_6}{\partial I_n} & 0 & 0 & 0 \\ 0 & \frac{\partial F_7}{\partial I_b} & \frac{\partial F_7}{\partial I_c} & 0 & 0 & 0 & \frac{\partial F_7}{\partial I_o} & \frac{\partial F_7}{\partial I_p} & 0 \\ 0 & \frac{\partial F_8}{\partial I_b} & \frac{\partial F_8}{\partial I_c} & 0 & 0 & 0 & \frac{\partial F_8}{\partial I_o} & \frac{\partial F_8}{\partial I_p} & 0 \\ 0 & 0 & \frac{\partial F_9}{\partial I_c} & \frac{\partial F_9}{\partial I_d} & 0 & 0 & 0 & 0 & \frac{\partial F_9}{\partial I_q} \end{array} \right]$$

and where the elements of \mathbf{J} are defined in Appendix A.

- 5) Estimate the correction current vector $\Delta \mathbf{I}^{(n)}$ by solving the linear system

$$\mathbf{J}^{(n)} \cdot \Delta \mathbf{I}^{(n)} = \mathbf{F}^{(n)}$$

- 6) Check whether the absolute value of each element in $\Delta \mathbf{I}^{(n)}$ is less than a given tolerance. If yes, stop.
- 7) Otherwise, adjust the current vector $\mathbf{I}^{(n)}$ as follows:

$$\mathbf{I}^{(n+1)} = \mathbf{I}^{(n)} - \Delta \mathbf{I}^{(n)}$$

- 8) Increment n by 1 and go to step 3.

6.4. Examples

Two examples are given to illustrate this optimization algorithm.

Example #1

$$L = 9.08840 \cdot 10^{-5} \text{ H}, \quad I_{\text{base}} = 1137.565 \text{ A}, \quad I_{\text{sat}} = 1.5 \text{ p.u.}, \quad I_{\text{max}} = 15.0 \text{ p.u.}$$

Using the above data, the optimization program yields the following results:

| | |
|---|----------------------------|
| $L_1 = 9.08840 \cdot 10^{-5} \text{ H}$ | $I_a = 1853.75 \text{ A}$ |
| $L_2 = 1.80852 \cdot 10^{-5} \text{ H}$ | $I_b = 2898.83 \text{ A}$ |
| $L_3 = 3.18004 \cdot 10^{-6} \text{ H}$ | $I_c = 5214.53 \text{ A}$ |
| $L_4 = 3.63107 \cdot 10^{-7} \text{ H}$ | $I_d = 10077.05 \text{ A}$ |
| $L_5 = 8.84719 \cdot 10^{-8} \text{ H}$ | |

where L_1, \dots, L_5 are the slopes (inductances) of the linear segments, and I_a, \dots, I_d are the current points at which the piecewise linear curve changes from one segment to another. A comparison between the actual nonlinear characteristic and its piecewise linear representation is shown in Figure 6.2.

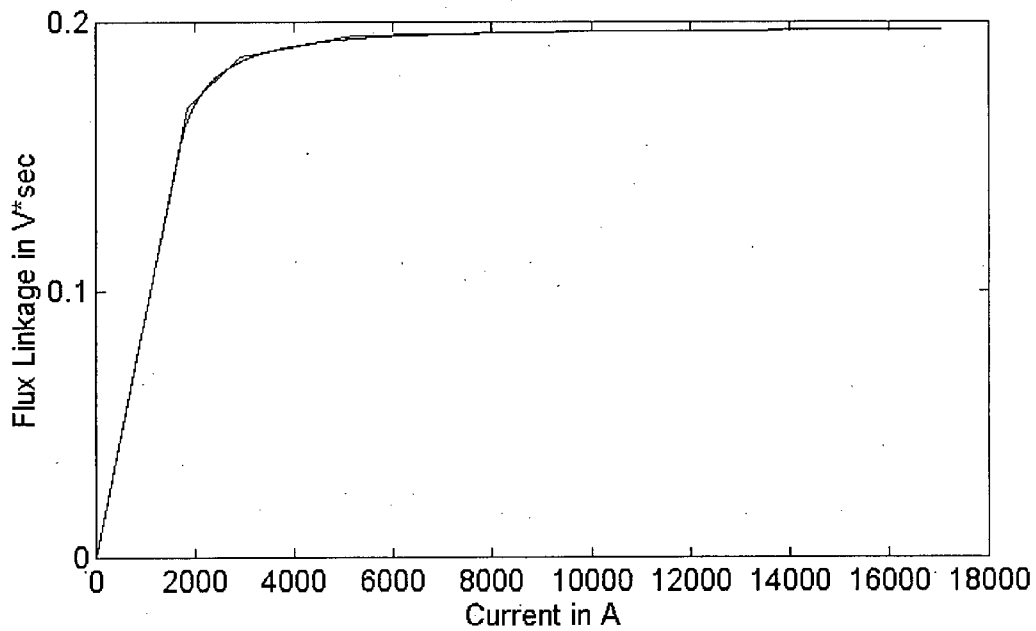


Figure 6.2 Comparison of the Saturation Characteristic and its Piecewise Linear Representation ($I_{\text{sat}} = 1.5 \text{ p.u.}$)

Example #2

$L = 9.08840 \cdot 10^{-5} \text{ H}$, $I_{\text{base}} = 1137.565 \text{ A}$, $I_{\text{sat}} = 3.0 \text{ p.u.}$, $I_{\text{max}} = 15.0 \text{ p.u.}$

Using the above data, the optimization program yields the following results:

| | |
|---|----------------------------|
| $L_1 = 9.08840 \cdot 10^{-5} \text{ H}$ | $I_a = 3639.39 \text{ A}$ |
| $L_2 = 2.43524 \cdot 10^{-5} \text{ H}$ | $I_b = 5087.09 \text{ A}$ |
| $L_3 = 6.50988 \cdot 10^{-6} \text{ H}$ | $I_c = 7773.70 \text{ A}$ |
| $L_4 = 1.41785 \cdot 10^{-6} \text{ H}$ | $I_d = 12036.04 \text{ A}$ |
| $L_5 = 5.38722 \cdot 10^{-7} \text{ H}$ | |

Again, L_1, \dots, L_5 are the slopes (inductances) of the linear segments, and I_a, \dots, I_d are the current points at which the piecewise linear curve changes from one segment to another. A comparison of the actual nonlinear characteristic and its piecewise linear representation is shown in Figure 6.3.

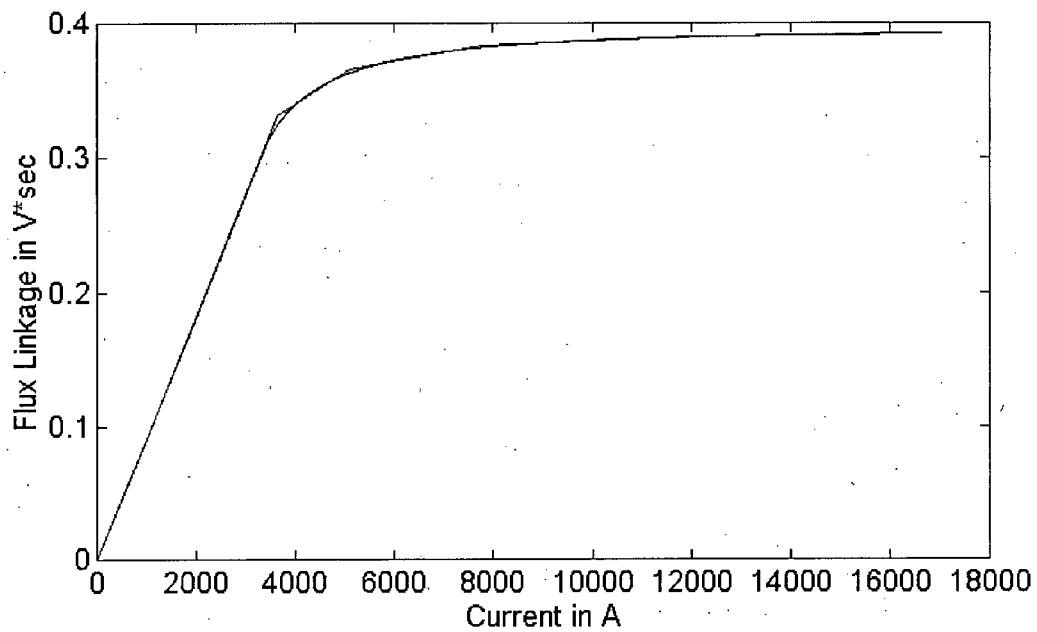


Figure 6.3 Comparison of the Saturation Characteristic and its Piecewise Linear Representation ($I_{\text{sat}} = 3.0$ p.u.)

Figures 6.2 and 6.3 show that the piecewise linear curves approximate the nonlinear characteristics very well.

CHAPTER 7

CASE STUDY

To show the usefulness of the proposed induction motor model, the start-up of a large induction motor is simulated. The supply network of the motor is represented as a Thevenin equivalent circuit, with a voltage of 6797.33 V (RMS, line-to-line), behind an inductance of $L_{pos} = 0.5305$ mH. The machine specifications are listed in Table 7.1.

Table 7.1 Specifications of the 11 000 HP Induction Motor [6]

Line-to-Line Voltage: 6600V

Full Load Specifications:

Efficiency = 0.985,
Power Factor = 0.906,
Rated Slip = 0.00622.

Starting Specifications:

at $V = 1.0$ p.u., $I = 8.0$ p.u.,
at $V = 0.758$ p.u., $I = 6.03$ p.u.,
Starting Torque = 1.457 p.u.

Other Information:

Maximum Torque = 3.5 p.u.,
Number of Poles = 4,
 $I_{sat} = 2.0$ p.u.,
Moment of Inertia = 50 590 lb·ft²,
Mechanical Load : $T_{mech} = 1.21 \cdot \omega^2$, where ω is the
machine speed in rad/sec.

Using the data conversion program described in Chapter 3, the following equivalent circuit parameters (in p.u.) are obtained:

$$\begin{aligned} R_s &= 4.586 \cdot 10^{-3}, & X_{so} &= 6.009 \cdot 10^{-2}, & X_{ss} &= 3.616 \cdot 10^{-3}, \\ X_m &= 3.094 \cdot 10^0, & X_{ro} &= 5.229 \cdot 10^{-2}, & X_{rs} &= 3.616 \cdot 10^{-3}, \\ R_1 &= 2.485 \cdot 10^{-2}, & R_2 &= 8.756 \cdot 10^{-3}, & X_2 &= 6.054 \cdot 10^{-2}. \end{aligned}$$

With the above data and $I_{\max} = 15.0$ p.u., the optimization program (described in Chapter 6) yields a piecewise linear curve with the following parameters:

$$\begin{aligned} L_1 &= 9.08840 \cdot 10^{-5} \text{ H} & I_a &= 2454.10 \text{ A} \\ L_2 &= 2.03003 \cdot 10^{-5} \text{ H} & I_b &= 3671.75 \text{ A} \\ L_3 &= 4.22453 \cdot 10^{-6} \text{ H} & I_c &= 6183.43 \text{ A} \\ L_4 &= 6.33421 \cdot 10^{-7} \text{ H} & I_d &= 10869.55 \text{ A} \\ L_5 &= 1.86161 \cdot 10^{-7} \text{ H} \end{aligned}$$

L_1, \dots, L_5 are the slopes (inductances) of the linear segments, and I_a, \dots, I_d are the current points at which the piecewise linear curve changes from one segment to another. The actual characteristic and its piecewise linear representation are shown in Figure 7.1. It is seen that the piecewise linear representation approximates the continuous characteristic very well.

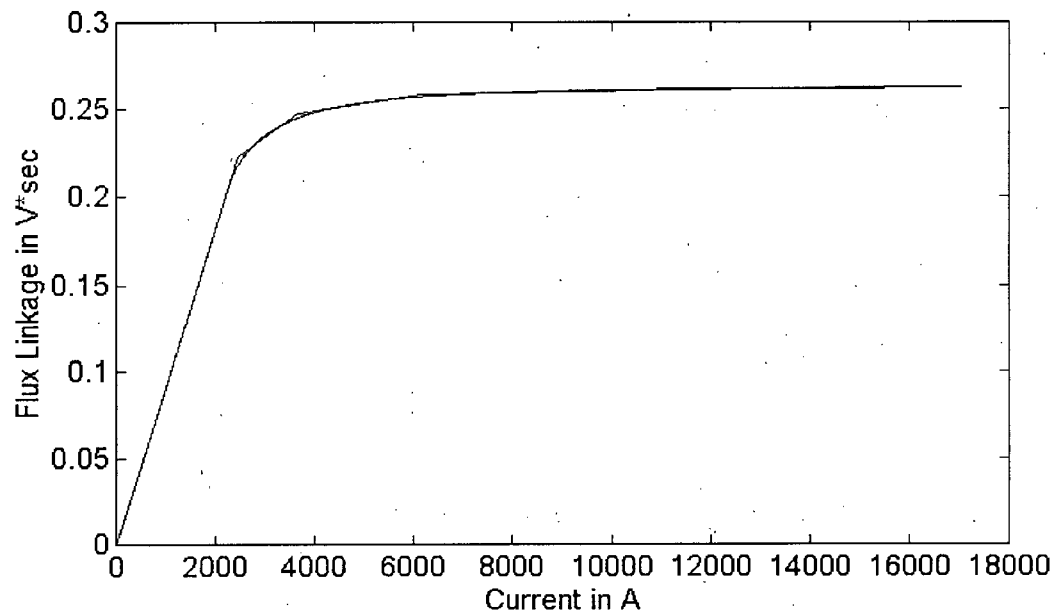


Figure 7.1. Comparison of the Continuous Saturation Curve and its Piecewise Linear Representation

The simulation results for the 11 000 HP induction motor during start-up are shown in Figure 7.2.

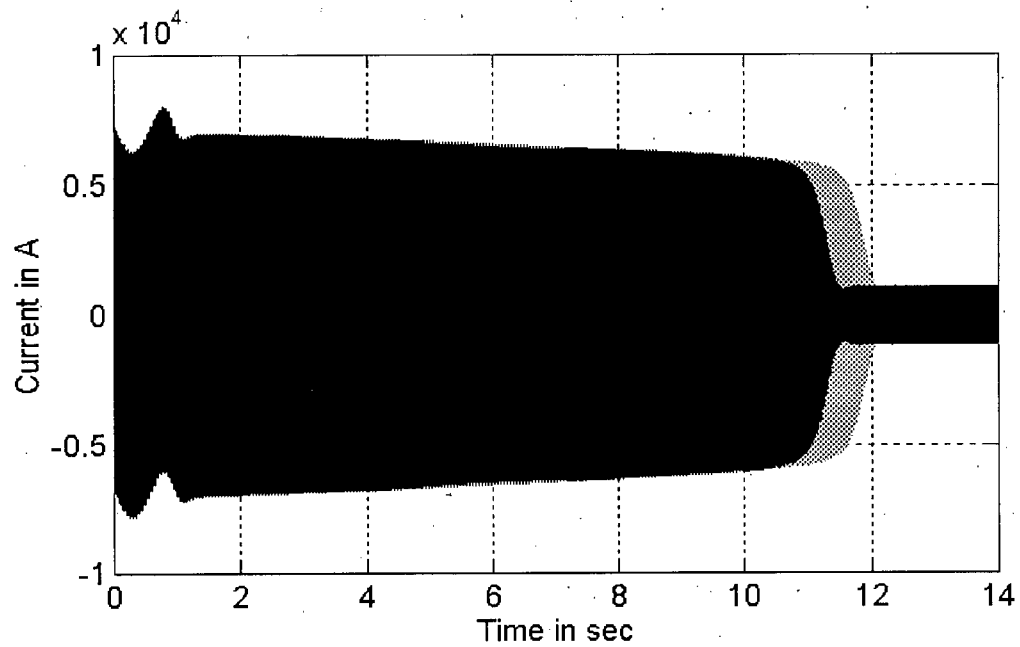


Figure 7.2(a) Current Envelope

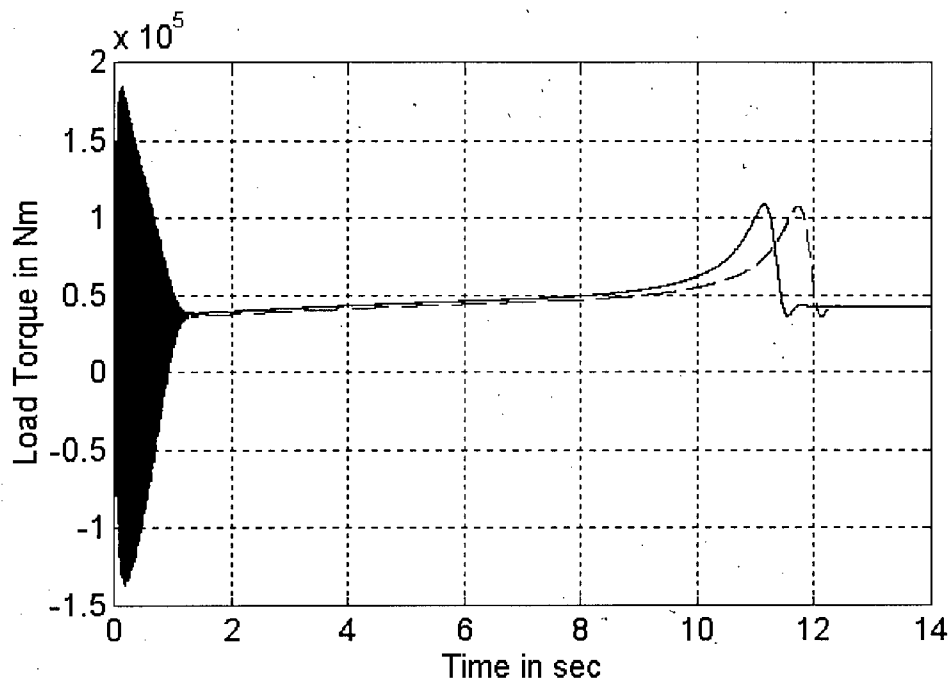


Figure 7.2(b) Torque Curve

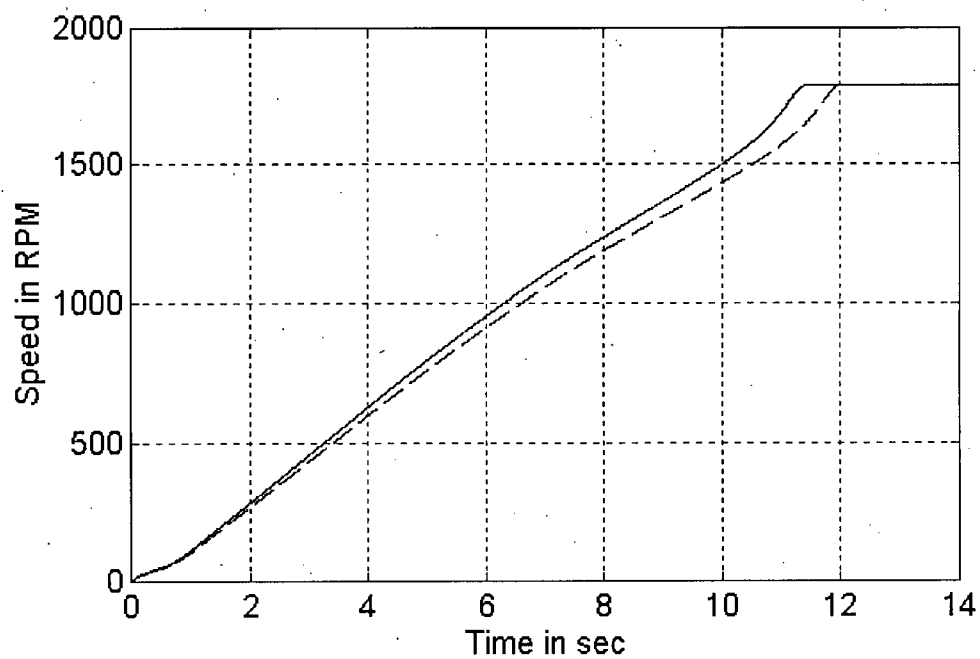


Figure 7.2(c) Speed Curve

Figure 7.2 Simulation Results for an Induction Motor During Start-Up

— Nonlinear Model - - - - Linear Model

The current envelope in Figure 7.2(a) shows the large inrush currents which exist during a motor start-up. The amplitudes of these currents remain practically unchanged until the motor has reached its rated speed. In addition, d.c. offset currents are present in the beginning of the start-up process. The torque curve, on the other hand, shows that the motor torque has large oscillations immediately after the motor is energized. Comparing Figures 7.2(a) and 7.2(b), it is seen that the oscillatory torque decays with the d.c. offset currents. Finally, the speed curve shows that the rotor speed climbs up steadily to its rated value. A small overshoot is observed before the rotor speed settles down to its rated value.

The results of Figure 7.2 have been obtained with MicroTran, and have been verified with an independent program, which uses a 4th-order Runge-Kutta solution method, as discussed in Chapter 5.

Figure 7.2 shows that the linear model overestimates the starting time of the motor, thus giving a pessimistic result. The saturable inductances are much smaller than their unsaturable counterparts ($L_{so}/L_{ss} \approx L_{ro}/L_{rs} \approx 15.0$); hence, the saturation effects are not very pronounced in this motor, as illustrated by the differences between the linear and nonlinear models. The saturation effects may be more noticeable in other motors.

To show the correctness of the proposed steady-state initialization methods, the behavior of this motor is simulated using the steady-state solution as initial conditions.

Using the Thevenin equivalent based method, the operating slip of this motor is found to be 0.005906. Using $\delta = 15^\circ$ (0.2618 in rad), and the procedures outlined in Section 4.4, the following steady-state solution is obtained:

$$I_d = 934.9506 \text{ A}$$

$$I_q = -975.2451 \text{ A}$$

$$I_o = 0.0 \text{ A}$$

$$I_f = -126.7777 \text{ A}$$

$$I_g = 297.8980 \text{ A}$$

$$I_D = -393.6692 \text{ A}$$

$$I_Q = 829.3784 \text{ A}$$

$$\omega = 374.7645 \text{ rad/s (electrical quantity)}$$

$$\beta(0) = 1.83260 \text{ rad (electrical quantity)}$$

This steady-state solution is then used as initial conditions for the transient simulation. The simulation results are shown in Figure 7.3.

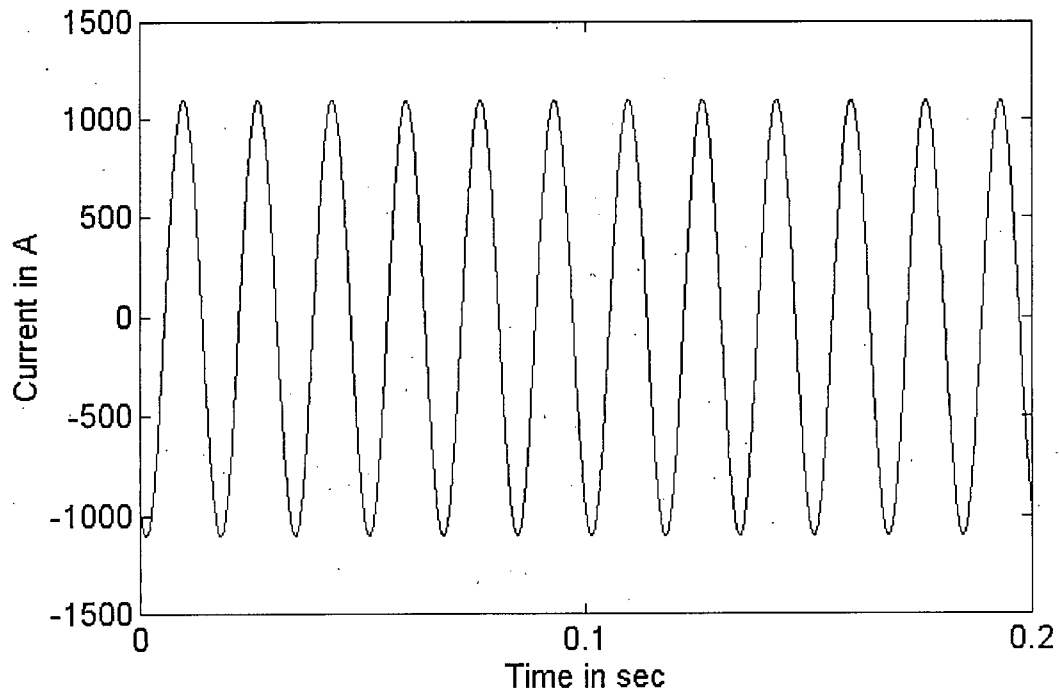


Figure 7.3(a) Current Waveform

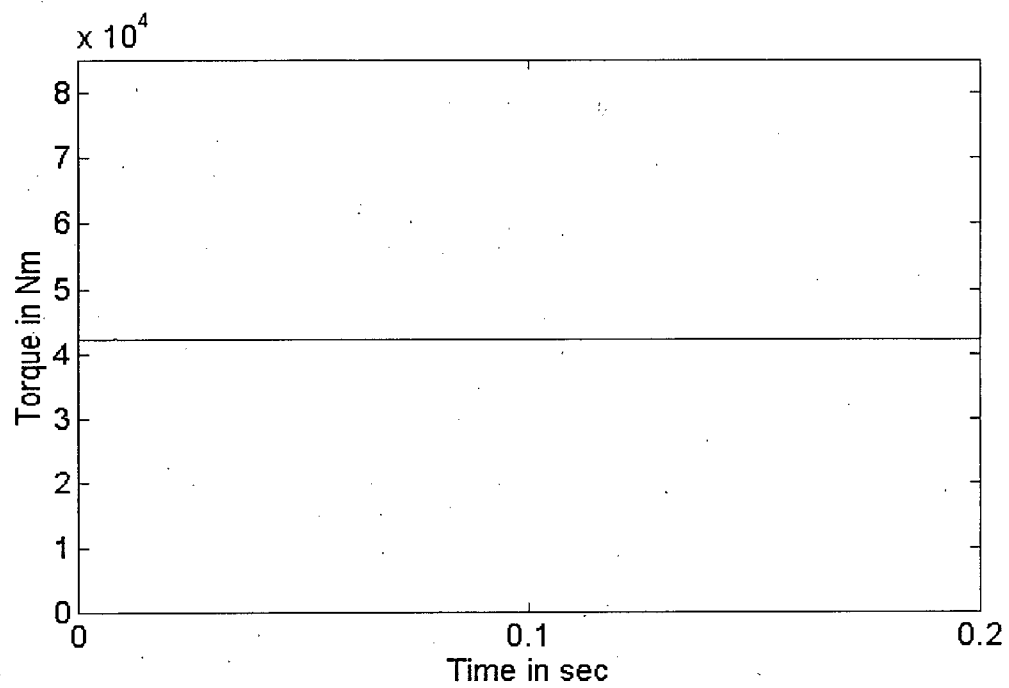


Figure 7.3(b) Torque Curve

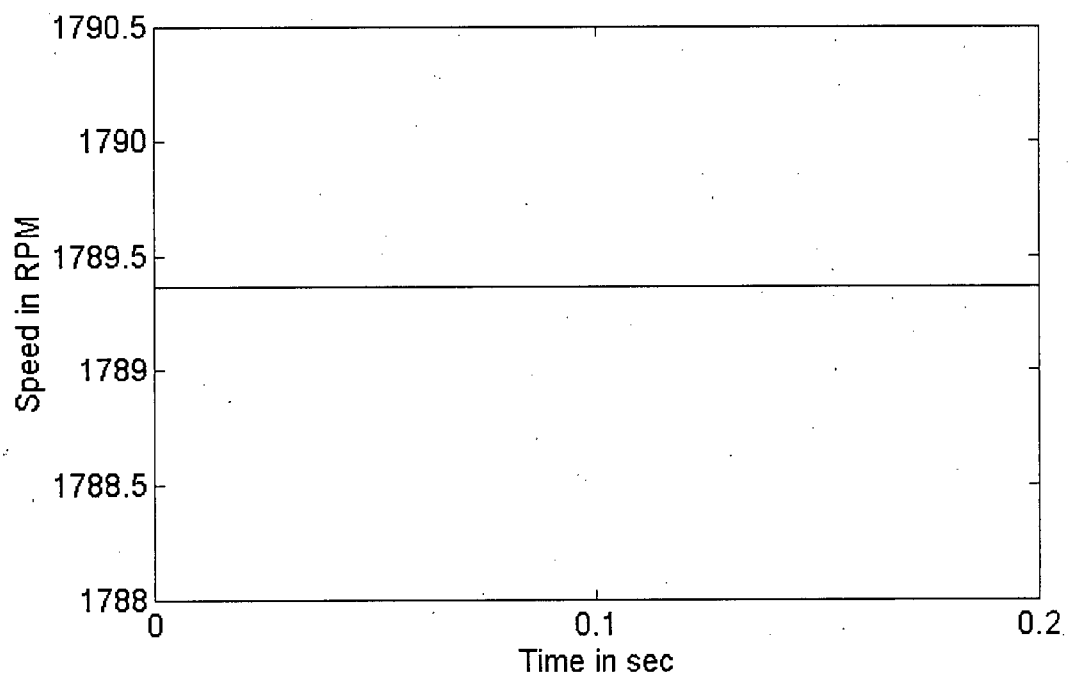


Figure 7.3(c) Speed Curve

Figure 7.3 Steady-State Behavior of an Induction Motor

Smooth transitions from the steady-state solution to the transient solution are observed in Figure 7.3. This indicates the correctness of the proposed initialization method.

CHAPTER 8

CONCLUSIONS

Induction motors form a considerable portion of industrial loads; hence, the analysis of their performance is often required in system studies. The Electromagnetic Transients Program (EMTP) is a computer program which can be used to simulate induction motor behavior. This thesis presents a method of using the EMTP synchronous machine model to simulate induction motor transients. This approach allows simulations of both machine types using essentially the same program code, making program maintenance easier.

A data conversion program which converts standard motor specifications into equivalent circuit parameters is explained. In this program, the design ratio is adjusted to meet the breakdown torque requirement. This approach is more effective than the one using the saturation threshold current [6].

Procedures for steady-state initialization are also discussed. Iterative algorithms for finding the operating slips of induction motors are presented as well. Examples of using these algorithms are given. The results suggest that the proposed algorithms converge very quickly to the solution.

Furthermore, the start-up of an induction motor is simulated using the proposed model. The simulation results from MicroTran agree very well with the results from the independent program discussed in this thesis.

Finally, an optimization algorithm for finding the best piecewise linear representation of the nonlinear saturation characteristic is discussed. Examples of using this algorithm are

given. The results show that the piecewise linear curves approximate the nonlinear characteristics very well.

REFERENCES

- [1] Electric Power Research Institute, EMTP Development Coordination Group, EPRI EL-6421-L : Electromagnetic Transients Program (EMTP) Revised Rule Book Version 2.0. Volume 1 : Main Program, June 1989.
- [2] A.M.A Mahmoud and R.W. Menzies, "A Complete Time Domain Model of the Induction Motor for Efficiency Evaluation", IEEE Trans. Energy Conversion, Vol. EC-1, pp. 68 - 76, Mar. 1986.
- [3] G. Andria, A. Dell'Aquila, L. Salvatore and M. Savino, "Improvement in Modeling and Testing of Induction Motors", IEEE Trans. Energy Conversion, Vol. EC-2, pp. 285 - 293. June 1987.
- [4] I.R. Smith and S. Sriharan, "Transients in Induction Machines with Terminal Capacitors", PROC. IEE, Vol. 115, pp. 519 - 527, Apr. 1968.
- [5] F.P. de Mello and G.W. Walsh, "Reclosing Transients in Induction Motors with Terminal Capacitors", AIEE Trans. PAS, Vol. 80, pp. 1206 - 1213, Feb. 1961.
- [6] G.J. Rogers and D. Shirmohammadi, "Induction Machine Modelling for Electromagnetic Transients Program", IEEE Trans. Energy Conversion, Vol. EC-2, pp. 622 - 628, Dec. 1987.
- [7] B.J. Chalmers and A.S. Mulki, "Design Synthesis of Double-Cage Induction Motors", PROC. IEE, Vol. 117, pp. 1257 - 1263, July 1970.
- [8] H.W. Dommel, *EMTP Theory Book, Second Edition*. MicroTran Power System Analysis Corporation, Vancouver, British Columbia, May 1992.
- [9] G.J. Rogers, J. Manno, and R. Alden, "An Aggregate Induction Motor Model for Industrial Plants", IEEE Trans. PAS, Vol. PAS-103, pp. 683 - 690, Apr. 1984.
- [10] R. Hung and H. W. Dommel, "Modelling of Induction Motors in the EMTP Using Existing Synchronous Machine Models", Trans. Engineering and Operating Division, Canadian Electrical Association, March 1995.
- [11] P. C. Sen, *Principle of Electric Machines and Power Electronics*, John Wiley & Sons., New York, 1989.

APPENDIX A

Definitions of the Elements in the Jacobian Matrix

The Jacobian matrix **J** in Section 6.3 is symmetric, and its elements are defined as follows:

$$\frac{\partial F_1}{\partial I_a} = L - M(I_m, I_n) \quad (A1)$$

$$\frac{\partial F_1}{\partial I_m} = -I_a \cdot \frac{\partial}{\partial I_m} M(I_m, I_n) - \frac{\partial}{\partial I_m} C(I_m, I_n) \quad (A2)$$

$$\frac{\partial F_1}{\partial I_n} = -I_a \cdot \frac{\partial}{\partial I_n} M(I_m, I_n) - \frac{\partial}{\partial I_n} C(I_m, I_n) \quad (A3)$$

$$\frac{\partial F_2}{\partial I_b} = M(I_m, I_n) - M(I_o, I_p) \quad (A4)$$

$$\frac{\partial F_2}{\partial I_m} = I_b \cdot \frac{\partial}{\partial I_m} M(I_m, I_n) + \frac{\partial}{\partial I_m} C(I_m, I_n) \quad (A5)$$

$$\frac{\partial F_2}{\partial I_n} = I_b \cdot \frac{\partial}{\partial I_n} M(I_m, I_n) + \frac{\partial}{\partial I_n} C(I_m, I_n) \quad (A6)$$

$$\frac{\partial F_2}{\partial I_o} = -I_b \cdot \frac{\partial}{\partial I_o} M(I_o, I_p) - \frac{\partial}{\partial I_o} C(I_o, I_p) \quad (A7)$$

$$\frac{\partial F_2}{\partial I_p} = -I_b \cdot \frac{\partial}{\partial I_p} M(I_o, I_p) - \frac{\partial}{\partial I_p} C(I_o, I_p) \quad (A8)$$

$$\frac{\partial F_3}{\partial I_c} = M(I_o, I_p) - M(I_q, I_d) \quad (A9)$$

$$\frac{\partial F_3}{\partial I_d} = -I_c \cdot \frac{\partial}{\partial I_d} M(I_q, I_d) - \frac{\partial}{\partial I_d} C(I_q, I_d) \quad (A10)$$

$$\frac{\partial F_3}{\partial I_o} = I_c \cdot \frac{\partial}{\partial I_o} M(I_o, I_p) + \frac{\partial}{\partial I_o} C(I_o, I_p) \quad (A11)$$

$$\frac{\partial F_3}{\partial I_p} = I_c \cdot \frac{\partial}{\partial I_p} M(I_o, I_p) + \frac{\partial}{\partial I_p} C(I_o, I_p) \quad (A12)$$

$$\frac{\partial F_3}{\partial I_q} = -I_c \cdot \frac{\partial}{\partial I_q} M(I_q, I_d) - \frac{\partial}{\partial I_q} C(I_q, I_d) \quad (A13)$$

$$\frac{\partial F_4}{\partial I_c} = \frac{\partial F_3}{\partial I_d} \quad (A14)$$

$$\begin{aligned} \frac{\partial F_4}{\partial I_d} = & 0.5 (2 I_q^2 - I_c^2 - I_d^2) \cdot \frac{\partial^2}{\partial I_d^2} M(I_q, I_d) + (2 I_q - I_c - I_d) \cdot \frac{\partial^2}{\partial I_d^2} C(I_q, I_d) \\ & - 2 \frac{\partial}{\partial I_d} C(I_q, I_d) + 2 I_d \cdot \frac{\partial}{\partial I_d} M(I_d, I_{\max}) - 2 I_d \cdot \frac{\partial}{\partial I_d} M(I_q, I_d) - M(I_q, I_d) \\ & + M(I_d, I_{\max}) - 0.5 (I_{\max}^2 - I_d^2) \cdot \frac{\partial^2}{\partial I_d^2} M(I_d, I_{\max}) + 2 \frac{\partial}{\partial I_d} C(I_d, I_{\max}) \\ & - (I_{\max} - I_d) \cdot \frac{\partial^2}{\partial I_d^2} C(I_d, I_{\max}) \end{aligned} \quad (A15)$$

$$\begin{aligned} \frac{\partial F_4}{\partial I_q} = & 2 I_q \cdot \frac{\partial}{\partial I_d} M(I_q, I_d) + 0.5 (2 I_q^2 - I_c^2 - I_d^2) \cdot \frac{\partial^2}{\partial I_q \partial I_d} M(I_q, I_d) \\ & + 2 \frac{\partial}{\partial I_d} C(I_q, I_d) + (2 I_q - I_c - I_d) \cdot \frac{\partial^2}{\partial I_q \partial I_d} C(I_q, I_d) - I_d \frac{\partial}{\partial I_q} M(I_q, I_d) \\ & - \frac{\partial}{\partial I_q} C(I_q, I_d) \end{aligned} \quad (A16)$$

$$\frac{\partial F_5}{\partial I_a} = \frac{\partial F_1}{\partial I_m} \quad (A17)$$

$$\frac{\partial F_5}{\partial I_b} = \frac{\partial F_2}{\partial I_m} \quad (A18)$$

$$\begin{aligned}
\frac{\partial F_5}{\partial I_m} &= 0.5 (2 I_m^2 - I_a^2 - 2 I_n^2 + I_b^2) \frac{\partial^2}{\partial I_m^2} M(I_m, I_n) + 4 I_m \frac{\partial}{\partial I_m} M(I_m, I_n) \\
&+ (2 I_m - I_a - 2 I_n + I_b) \frac{\partial^2}{\partial I_m^2} C(I_m, I_n) + 4 \frac{\partial}{\partial I_m} C(I_m, I_n) - 2 \lambda'(I_m) \\
&+ 2 M(I_m, I_n)
\end{aligned} \tag{A19}$$

$$\begin{aligned}
\frac{\partial F_5}{\partial I_n} &= 0.5 (2 I_m^2 - I_a^2 - 2 I_n^2 + I_b^2) \frac{\partial^2}{\partial I_n \partial I_m} M(I_m, I_n) + 2 I_m \frac{\partial}{\partial I_n} M(I_m, I_n) \\
&+ (2 I_m - I_a - 2 I_n + I_b) \frac{\partial^2}{\partial I_n \partial I_m} C(I_m, I_n) + 2 \frac{\partial}{\partial I_n} C(I_m, I_n) \\
&- 2 \frac{\partial}{\partial I_m} C(I_m, I_n) - 2 I_n \frac{\partial}{\partial I_m} M(I_m, I_n)
\end{aligned} \tag{A20}$$

$$\frac{\partial F_6}{\partial I_a} = \frac{\partial F_1}{\partial I_n} \tag{A21}$$

$$\frac{\partial F_6}{\partial I_b} = \frac{\partial F_2}{\partial I_n} \tag{A22}$$

$$\frac{\partial F_6}{\partial I_m} = \frac{\partial F_5}{\partial I_n} \tag{A23}$$

$$\begin{aligned}
\frac{\partial F_6}{\partial I_n} &= 0.5 (2 I_m^2 - I_a^2 - 2 I_n^2 + I_b^2) \frac{\partial^2}{\partial I_n^2} M(I_m, I_n) - 4 I_n \frac{\partial}{\partial I_n} M(I_m, I_n) \\
&+ (2 I_m - I_a - 2 I_n + I_b) \frac{\partial^2}{\partial I_n^2} C(I_m, I_n) - 4 \frac{\partial}{\partial I_n} C(I_m, I_n) + 2 \lambda'(I_n) \\
&- 2 M(I_m, I_n)
\end{aligned} \tag{A24}$$

$$\frac{\partial F_7}{\partial I_b} = \frac{\partial F_2}{\partial I_o} \tag{A25}$$

$$\frac{\partial F_7}{\partial I_c} = \frac{\partial F_3}{\partial I_o} \quad (A26)$$

$$\begin{aligned} \frac{\partial F_7}{\partial I_o} = & 0.5 (2 I_o^2 - I_b^2 - 2 I_p^2 + I_c^2) \frac{\partial^2}{\partial I_o^2} M(I_o, I_p) + 4 I_o \frac{\partial}{\partial I_o} M(I_o, I_p) \\ & + (2 I_o - I_b - 2 I_p + I_c) \frac{\partial^2}{\partial I_o^2} C(I_o, I_p) + 4 \frac{\partial}{\partial I_o} C(I_o, I_p) - 2 \lambda'(I_o) \\ & + 2 M(I_o, I_p) \end{aligned} \quad (A27)$$

$$\begin{aligned} \frac{\partial F_7}{\partial I_p} = & 0.5 (2 I_o^2 - I_b^2 - 2 I_p^2 + I_c^2) \frac{\partial^2}{\partial I_p \partial I_o} M(I_o, I_p) + 2 I_o \frac{\partial}{\partial I_p} M(I_o, I_p) \\ & + (2 I_o - I_b - 2 I_p + I_c) \frac{\partial^2}{\partial I_p \partial I_o} C(I_o, I_p) + 2 \frac{\partial}{\partial I_p} C(I_o, I_p) \\ & - 2 \frac{\partial}{\partial I_o} C(I_o, I_p) - 2 I_p \frac{\partial}{\partial I_o} M(I_o, I_p) \end{aligned} \quad (A28)$$

$$\frac{\partial F_8}{\partial I_b} = \frac{\partial F_2}{\partial I_p} \quad (A29)$$

$$\frac{\partial F_8}{\partial I_c} = \frac{\partial F_3}{\partial I_p} \quad (A30)$$

$$\frac{\partial F_8}{\partial I_o} = \frac{\partial F_7}{\partial I_p} \quad (A31)$$

$$\begin{aligned} \frac{\partial F_8}{\partial I_p} = & 0.5 (2 I_o^2 - I_b^2 - 2 I_p^2 + I_c^2) \frac{\partial^2}{\partial I_p^2} M(I_o, I_p) - 4 I_p \frac{\partial}{\partial I_p} M(I_o, I_p) \\ & + (2 I_o - I_b - 2 I_p + I_c) \frac{\partial^2}{\partial I_p^2} C(I_o, I_p) - 4 \frac{\partial}{\partial I_p} C(I_o, I_p) + 2 \lambda'(I_p) \\ & - 2 M(I_o, I_p) \end{aligned} \quad (A32)$$

$$\frac{\partial F_9}{\partial I_c} = \frac{\partial F_3}{\partial I_q} \quad (\text{A33})$$

$$\frac{\partial F_9}{\partial I_d} = \frac{\partial F_4}{\partial I_q} \quad (\text{A34})$$

$$\begin{aligned} \frac{\partial F_9}{\partial I_q} = & 0.5 (2 I_q^2 - I_c^2 - I_d^2) \frac{\partial^2}{\partial I_q^2} M(I_q, I_d) + 4 I_q \frac{\partial}{\partial I_q} M(I_q, I_d) \\ & + (2 I_q - I_c - I_d) \frac{\partial^2}{\partial I_q^2} C(I_q, I_d) + 4 \frac{\partial}{\partial I_q} C(I_q, I_d) \\ & + 2 M(I_q, I_d) - 2 \lambda'(I_q) \end{aligned} \quad (\text{A35})$$

where

$$\frac{\partial}{\partial I_1} M(I_1, I_2) = [\lambda(I_2) - \lambda(I_1) - \lambda'(I_1) \cdot (I_2 - I_1)] / (I_2 - I_1)^2 \quad (\text{A36})$$

$$\frac{\partial}{\partial I_2} M(I_1, I_2) = [\lambda(I_1) - \lambda(I_2) + \lambda'(I_2) \cdot (I_2 - I_1)] / (I_2 - I_1)^2 \quad (\text{A37})$$

$$\frac{\partial}{\partial I_1} C(I_1, I_2) = I_2 \cdot \{ \lambda'(I_1) \cdot [I_2 - I_1] - \lambda(I_2) + \lambda(I_1) \} / (I_2 - I_1)^2 \quad (\text{A38})$$

$$\frac{\partial}{\partial I_2} C(I_1, I_2) = I_1 \cdot \{ \lambda'(I_2) \cdot [I_1 - I_2] - \lambda(I_1) + \lambda(I_2) \} / (I_2 - I_1)^2 \quad (\text{A39})$$

$$\begin{aligned} \frac{\partial^2}{\partial I_1^2} M(I_1, I_2) = & \{ -\lambda''(I_1) \cdot (I_2 - I_1)^2 + 2 [\lambda(I_2) - \lambda(I_1) - \lambda'(I_1) \cdot (I_2 - I_1)] \} \\ & / (I_2 - I_1)^3 \end{aligned} \quad (\text{A40})$$

$$\frac{\partial^2}{\partial I_2^2} M(I_1, I_2) = \{ \lambda''(I_2) \cdot (I_2 - I_1)^2 - 2 [\lambda(I_1) - \lambda(I_2) + \lambda'(I_2) \cdot (I_2 - I_1)] \} / (I_2 - I_1)^3 \quad (A41)$$

$$\frac{\partial^2}{\partial I_1^2} C(I_1, I_2) = I_2 \cdot \{ \lambda''(I_1) \cdot (I_2 - I_1)^2 + 2 [\lambda'(I_1) \cdot (I_2 - I_1) - \lambda(I_2) + \lambda(I_1)] \} / (I_2 - I_1)^3 \quad (A42)$$

$$\frac{\partial^2}{\partial I_2^2} C(I_1, I_2) = I_1 \cdot \{ -\lambda''(I_2) \cdot (I_2 - I_1)^2 - 2 [\lambda'(I_2) \cdot (I_1 - I_2) - \lambda(I_1) + \lambda(I_2)] \} / (I_2 - I_1)^3 \quad (A43)$$

$$\frac{\partial^2}{\partial I_1 \partial I_2} M(I_1, I_2) = \{ (I_2 - I_1) \cdot [\lambda'(I_2) + \lambda'(I_1)] - 2 \cdot [\lambda(I_2) - \lambda(I_1)] \} / (I_2 - I_1)^3 \quad (A44)$$

$$\begin{aligned} \frac{\partial^2}{\partial I_1 \partial I_2} C(I_1, I_2) = & \{ \lambda'(I_1) \cdot (I_2 - I_1)^2 + (I_1 + I_2) \cdot [\lambda(I_2) - \lambda(I_1)] \\ & - I_2 \cdot (I_2 - I_1) \cdot [\lambda'(I_1) + \lambda'(I_2)] \} / (I_2 - I_1)^3 \end{aligned} \quad (A45)$$

also

$$\frac{\partial^2}{\partial I_1 \partial I_2} M(I_1, I_2) = \frac{\partial^2}{\partial I_2 \partial I_1} M(I_1, I_2) \quad (A46)$$

and

$$\frac{\partial^2}{\partial I_1 \partial I_2} C(I_1, I_2) = \frac{\partial^2}{\partial I_2 \partial I_1} C(I_1, I_2) \quad (A47)$$

Since $\lambda = L \cdot DF(i) \cdot i$ (A48)

$$\lambda' = L \{ DF(i) + DF'(i) \cdot i \}$$

where $DF'(i) = 0$ if $i \leq I_{sat}$

$$DF'(i) = (2/\pi) \cdot [A + B] \quad \text{if } i > I_{sat}$$

with $A = -I_{sat} / (R \cdot i^2)$

$$B = -I_{sat} \cdot R / i^2 + I_{sat}^3 / (R \cdot i^4)$$

where $R = [1 - (I_{sat}/i)^2]^{0.5}$ (A49)

and

$$\lambda'' = L \{ 2 \cdot DF'(i) + DF''(i) \cdot i \}$$

where $DF''(i) = 0$ if $i \leq I_{sat}$

$$DF''(i) = (2/\pi) \cdot [C + D] \quad \text{if } i > I_{sat}$$

with $C = 2 \cdot I_{sat} / (R \cdot i^3) + I_{sat}^3 / (R^3 \cdot i^5)$

$$D = 2 \cdot I_{sat} \cdot R / i^3 - I_{sat}^5 / (R^3 \cdot i^7) - 5 \cdot I_{sat}^3 / (R \cdot i^5)$$

where $R = [1 - (I_{sat}/i)^2]^{0.5}$ (A50)